Cell Reports
Article

Nkx6.1 Is Essential for Maintaining the Functional State of Pancreatic Beta Cells

Brandon L. Taylor,[1] Fen-Fen Liu,[1] and Maike Sander[1,*]
[1]Departments of Pediatrics and Cellular and Molecular Medicine, Pediatric Diabetes Research Center, University of California, San Diego, La Jolla, CA 92093-0695, USA
*Correspondence: masander@ucsd.edu
http://dx.doi.org/10.1016/j.celrep.2013.08.010

SUMMARY

Recently, loss of beta-cell-specific traits has been proposed as an early cause of beta cell failure in diabetes. However, the molecular mechanisms that underlie the loss of beta cell features remain unclear. Here, we identify an Nkx6.1-controlled gene regulatory network as essential for maintaining the functional and molecular traits of mature beta cells. Conditional *Nkx6.1* inactivation in adult mice caused rapid-onset diabetes and hypoinsulinemia. Genome-wide analysis of Nkx6.1-regulated genes and functional assays further revealed a critical role for Nkx6.1 in the control of insulin biosynthesis, insulin secretion, and beta cell proliferation. Over time, Nkx6.1-deficient beta cells acquired molecular characteristics of delta cells, revealing a molecular link between impaired beta cell functional properties and loss of cell identity. Given that Nkx6.1 levels are reduced in human type 2 diabetic beta cells, our study lends support to the concept that loss of beta cell features could contribute to the pathogenesis of diabetes.

INTRODUCTION

Type 2 diabetes mellitus (T2D) is characterized by reduced insulin sensitivity of insulin target tissues and impaired insulin secretion by pancreatic beta cells. Although both of these factors play a role, genetic studies suggest that the ability of beta cells to respond to metabolic stressors is the predominant factor in determining the predisposition to T2D (Muoio and Newgard, 2008).

In T2D, beta cells exhibit an impaired capacity to compensate for increased insulin demand (Cerasi and Luft, 1967), a defect that has been ascribed to both inadequate cellular capacity to secrete insulin (Hosker et al., 1989) and beta cell death (Butler et al., 2003). Among the earliest defects observed in T2D patients is a reduced ability of beta cells to secrete insulin in response to elevated blood glucose levels (Hosker et al., 1989). This impairment in glucose-stimulated insulin secretion has been attributed to defects in glucose sensing (Froguel et al., 1992), mitochondrial dysfunction (Supale et al., 2012), and oxidative stress (Robertson, 2004). Thus, mounting evidence suggests that defects in multiple cellular processes can compromise beta cell function and could be a factor in T2D development. Furthermore, hyperglycemia has been shown to impair the expression of genes that are important for beta cell identity (Jonas et al., 1999). More recently, Talchai et al. (2012) described a loss of beta cell features, characterized by a decline in insulin production, acquisition of progenitor-like characteristics, and fate conversion into other endocrine cell types in mouse models of T2D, suggesting that loss of the differentiated beta cell state also contributes to beta cell failure in T2D. However, it is currently unknown whether the loss of beta cell functional properties (namely, regulated insulin secretion) and loss of beta cell identity are linked during T2D progression. A simultaneous loss of beta cell function and identity could be explained by reduced expression of a central transcriptional regulator controlling genes involved in both processes.

Several lines of evidence suggest that the beta-cell-enriched transcription factor Nkx6.1 could have a role in T2D. First, genome-wide association studies suggest that variants of *Nkx6.1* associate with T2D (Yokoi et al., 2006). Second, decreased Nkx6.1 expression has been shown to accompany the development of T2D in rodents and humans (Guo et al., 2013; Talchai et al., 2012). Third, in vitro studies in beta cell lines and isolated islets suggest a possible role for Nkx6.1 in the regulation of glucose-stimulated insulin secretion as well as beta cell proliferation (Schisler et al., 2005, 2008). Additionally, we recently showed that Nkx6.1 is necessary and sufficient to confer beta cell identity to differentiating endocrine precursors in the embryo (Schaffer et al., 2013), raising the possibility that Nkx6.1 could also help maintain the differentiated state of adult beta cells. Together, these findings suggest that Nkx6.1 may be a regulator of beta cell function and identity in adult animals.

To explore the role of Nkx6.1 in mature beta cells, we ablated *Nkx6.1* specifically in beta cells of adult mice and identified Nkx6.1 target genes in beta cells by combining gene-expression profiling and chromatin immunoprecipitation with massively parallel sequencing (ChIP-seq). We found that loss of Nkx6.1 caused rapid-onset diabetes due to defects in insulin biosynthesis and secretion. The observed loss in insulin production and beta cell functional properties was later accompanied by ectopic activation of delta cell genes in beta cells. Thus, by impairing beta cell function and destabilizing beta cell identity,

reduced Nkx6.1 levels, as seen in T2D, could contribute to the pathogenesis of T2D.

RESULTS

Loss of Nkx6.1 in Mature Beta Cells Causes Diabetes and Reduced Insulin Production

To examine Nkx6.1 function in mature beta cells in vivo, we conditionally inactivated *Nkx6.1* in islet cells of adult mice by triggering recombination of an *Nkx6.1*^{flox} (*Nkx6.1*^{fl}) allele with the tamoxifen-inducible *Pdx1-CreER*^{TM} transgene. *Pdx1-CreER*^{TM}*;Nkx6.1*$^{fl/-}$ and *Pdx1-CreER*^{TM}*;Nkx6.1*$^{fl/+}$ mice were injected with tamoxifen between 4 and 6 weeks of age to produce *Nkx6.1*$^{\Delta adult\beta}$ and control mice, respectively (Figures 1A and 1B). Quantitative RT-PCR (qRT-PCR) and immunofluorescence staining for Nkx6.1 demonstrated efficient recombination of the *Nkx6.1*^{fl} allele in beta cells (Figures 1C, 1I, and 1J).

To determine whether *Nkx6.1* deletion affects beta cell function, we conducted glucose tolerance tests and measured blood glucose levels. Glucose tolerance tests performed 1 week after the last tamoxifen injection revealed elevated fasting blood glucose levels and glucose intolerance in male *Nkx6.1*$^{\Delta adult\beta}$ mice when compared with tamoxifen-treated and non-tamoxifen-treated control mice (Figure 1D). Likewise, blood glucose levels were significantly elevated in *Nkx6.1*$^{\Delta adult\beta}$ mice fed ad libitum, with levels reaching near 500 mg/dl within 8 weeks after the last tamoxifen injection (Figure 1E). Female *Nkx6.1*$^{\Delta adult\beta}$ mice also became diabetic, but the phenotype developed slightly later and was less severe than in males (Figures S1A–S1C). Thus, loss of Nkx6.1 in adult beta cells causes rapid development of diabetes.

To investigate whether diabetes in *Nkx6.1*$^{\Delta adult\beta}$ mice is caused by insulin insufficiency, we measured plasma insulin levels after glucose administration. As expected, control mice responded to a glucose bolus with a rapid increase in plasma insulin levels within 5 min of glucose administration (Figure 1F). By contrast, insulin levels did not increase in *Nkx6.1*$^{\Delta adult\beta}$ mice and blood glucose levels were significantly higher than in control mice (Figures 1F and 1G). A striking reduction in pancreatic insulin content in *Nkx6.1*$^{\Delta adult\beta}$ mice (Figure 1H) further demonstrated decreased overall pancreatic insulin production. To determine whether the reduction in pancreatic insulin levels in *Nkx6.1*$^{\Delta adult\beta}$ mice is a result of beta cell loss, we next examined beta cell survival and quantified beta cell mass. *Nkx6.1*$^{\Delta adult\beta}$ mice did not show increased beta cell apoptosis (Figures S2A–S2D) or reduced mass of endocrine or beta cells (Figures S2E–S2H), suggesting that diabetes in *Nkx6.1*$^{\Delta adult\beta}$ mice is caused by decreased insulin biosynthesis rather than beta cell loss. Consistent with a possible defect in the cellular production of insulin, the insulin fluorescence signal was dramatically reduced in Nkx6.1-deficient beta cells (Figures 1I and 1J). Notably, reduced insulin production did not appear to be accompanied by a change in endocrine cell type identity, as insulin^{+} cells in *Nkx6.1*$^{\Delta adult\beta}$ mice did not coexpress other pancreatic hormones (Figures S2I–S2N). These data suggest that diabetes following *Nkx6.1* inactivation is initially caused at least in part by loss of insulin production, but not by cell death or conversion into other endocrine cell types.

Nkx6.1 Directly Regulates Islet Transcription Factors and Genes Involved in Glucose Metabolism and Insulin Biosynthesis

To more globally understand how loss of Nkx6.1 impacts beta cell gene expression, and to identify molecular pathways that are immediately affected following *Nkx6.1* inactivation, we next conducted transcriptional profiling of *Nkx6.1*$^{\Delta adult\beta}$ and control islets 3 days after completion of tamoxifen-induced *Nkx6.1* ablation (Figure 2A). At this time point, *Nkx6.1*$^{\Delta adult\beta}$ mice were only mildly glucose intolerant and blood glucose levels of mice fed ad libitum were still below 250 mg/dl (Figures S3A and S3B). A comparison of gene-expression profiles between *Nkx6.1*$^{\Delta adult\beta}$ and control islets revealed significant differences in the expression of 1,455 genes (false discovery rate [FDR] < 0.01 and fold change [FC] > 1.5; Table S1), of which 887 were upregulated and 568 were downregulated. To define the cellular processes affected by *Nkx6.1* inactivation, we performed Gene Ontology (GO) analysis of the differentially expressed genes. Consistent with the diabetic phenotype, Nkx6.1-regulated genes showed association with biological processes that are critical for beta cell function, such as ion transport, regulation of secretion, oxidation reduction, insulin secretion, and hexose biosynthesis (Figure 2B). These data suggest that reduced insulin production may not be the only cause of hyperglycemia following *Nkx6.1* deletion, and that simultaneous impairment of multiple processes required for proper beta cell function could contribute to the development of diabetes in *Nkx6.1*$^{\Delta adult\beta}$ mice.

To distinguish between direct transcriptional target genes of Nkx6.1 and genes indirectly affected by *Nkx6.1* inactivation, we performed ChIP-seq for Nkx6.1 on primary mouse islets to identify Nkx6.1-occupied genes. We detected a total of 6,771 Nkx6.1 binding regions throughout the murine genome (FDR < 0.001; Table S2), 4,066 of which were near genes or intronic (Figure 2C). De novo motif analysis revealed a TAAT core motif and two flanking nucleotides on each side as the sequence motif preferentially occupied by Nkx6.1 (Figure 2D). Notably, the TAAT core of the Nkx6.1 de novo binding motif was previously identified by an in vitro electrophoretic mobility shift assay (Jørgensen et al., 1999). The TAAT motif is shared among many homeodomain transcription factors (Wilson et al., 1996), demonstrating binding of Nkx6.1 to the core homeodomain-binding motif.

Next, to determine the overlap between the genes occupied by Nkx6.1 in beta cells and genes whose expression is affected by Nkx6.1 loss, we analyzed which of the 1,988 Nkx6.1 binding sites within 10 kb of a transcriptional start site were associated with genes significantly regulated in Nkx6.1-deficient islets. Surprisingly, only 8% of Nkx6.1-occupied genes (135/1,818) were also regulated by Nkx6.1 (Figure 2E; Table S3). Similarly, of the 1,455 genes with statistically significant changes in expression, only 9% were bound by Nkx6.1 (Figure 2E), indicating that only a fraction of the genes affected by *Nkx6.1* inactivation depend directly on transcriptional input by Nkx6.1. Statistical analysis using hypergeometric distribution (Bhinge et al., 2007) revealed that this overlap between Nkx6.1-bound and -regulated genes was still significantly greater than randomly expected ($p < 0.05$). Interestingly, an equal percentage of Nkx6.1-bound and -regulated genes were upregulated as were downregulated

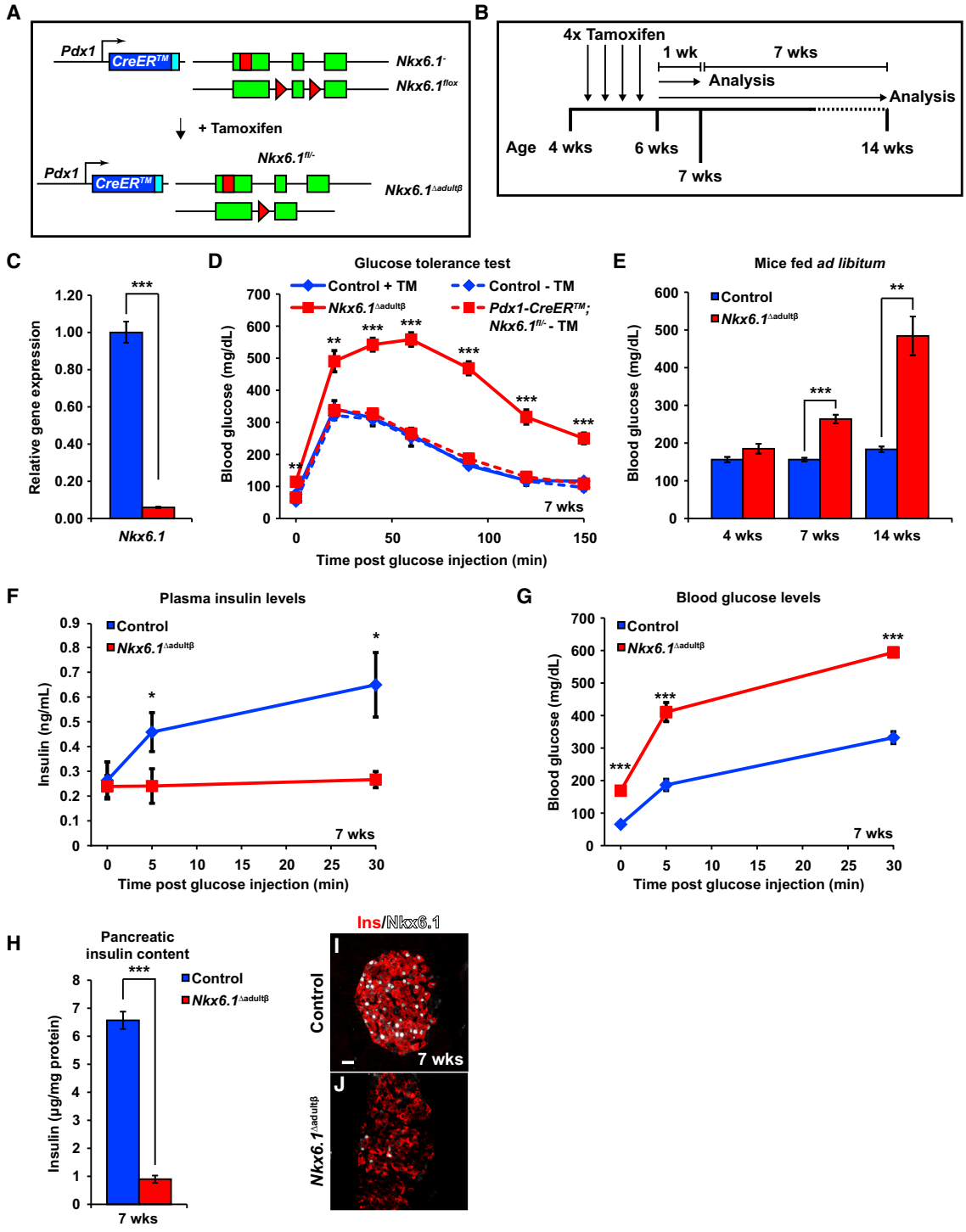

Figure 1. Deletion of *Nkx6.1* in Adult Beta Cells Results in Diabetes and Loss of Pancreatic Insulin

(A) Schematic of alleles and transgenes used to inactivate *Nkx6.1* in adult beta cells. Rectangles: coding sequences; triangles: *loxP* sites.

(B) Schematic of the experimental design. wks, weeks.

(C) qRT-PCR analysis of isolated islets shows a significant reduction of *Nkx6.1* in *Nkx6.1*$^{\Delta adult\beta}$ mice (n = 3).

(D) Intraperitoneal glucose tolerance test reveals glucose intolerance in male *Nkx6.1*$^{\Delta adult\beta}$ mice compared with noninjected and tamoxifen (TM)-treated control mice at 7 weeks (n = 6). Solid lines: post-TM treatment; dashed lines: without TM treatment.

(E) Blood glucose measurements of mice fed ad libitum show diabetes in male *Nkx6.1*$^{\Delta adult\beta}$ mice (n = 6).

(F and G) *Nkx6.1*$^{\Delta adult\beta}$ mice have lower plasma insulin levels and elevated blood glucose after a glucose stimulus compared with control mice (n = 6).

(legend continued on next page)

(Figures 2F and 2G), suggesting that Nkx6.1 can act as both a transcriptional repressor and activator.

Nkx6.1 was found to directly regulate various critical beta cell genes, including genes involved in glucose uptake and metabolism (*Slc2a2* [*Glut2*], *Pcx*, and *G6pc2*) and insulin processing (*Ero1lb* and *Slc30a8*), as well as transcriptional regulators with known roles in islet development and/or beta cell function (*MafA*, *Rfx6*, *Mnx1*, and *Tle3*; Figure 2E). These results suggest that Nkx6.1 exerts its function by transcriptionally regulating mediators of multiple beta cell processes.

The Insulin Secretory Response Is Impaired after *Nkx6.1* Inactivation

The insulin secretory response of beta cells is regulated by the coupling of glucose metabolism to insulin secretion (Muoio and Newgard, 2008). Glycolysis results in an increase in the ATP:ADP ratio, which serves as the key trigger for closure of ATP-sensitive potassium channels (K_{ATP} channels), ultimately stimulating calcium influx and insulin secretion. Because Nkx6.1 directly regulates the glucose metabolic genes *Glut2*, *Pcx*, and *G6pc2* (Table S1; Figures 3A–3C), we hypothesized that glucose uptake, glycolytic flux, and energy production could be impaired in Nkx6.1-deficient beta cells. Supporting the conclusion that the downregulation of Glut2 is physiologically significant, we found that *Nkx6.1*$^{\Delta adult\beta}$ mice were resistant to streptozotocin-induced beta cell death (data not shown), which depends on Glut2-mediated uptake of streptozotocin (Schnedl et al., 1994).

To investigate whether the changes in expression of glucose metabolic genes are associated with defects in energy production, we stained pancreata for phospho-AMP kinase (p-AMPK), a sensitive indicator of cellular energy depletion (low ATP:AMP ratio; Porat et al., 2011). *Nkx6.1*$^{\Delta adult\beta}$ islets displayed strikingly more intense p-AMPK staining than control islets (Figures 3D–3E′), indicating that loss of Nkx6.1 causes reduced glycolytic flux and energy stress. Further supporting this conclusion, intracellular ATP content was also significantly decreased in *Nkx6.1*$^{\Delta adult\beta}$ islets (Figure 3F). We conclude that despite increased blood glucose levels, Nkx6.1 deficiency results in energy-depleted beta cells. Since energy depletion has been shown to impair insulin secretion and cause diabetes in mice (Piston et al., 1999; Porat et al., 2011; Terauchi et al., 1995), the defect in energy production in *Nkx6.1*$^{\Delta adult\beta}$ mice could lead to a severely impaired insulin secretory response.

In addition to affecting ATP production, *Nkx6.1* deletion also led to reduced expression of *Sytl4*, a vesicle-associated protein that has been implicated in the modulation of insulin secretion (Gomi et al., 2005), as well as *Ucn3* and *Glp1r* (Figures 3G–3I), which are involved in peptide-mediated potentiation of insulin secretion (Li et al., 2007; Preitner et al., 2004). These changes in gene expression suggest that Nkx6.1 also has glucose-metabolism-independent roles in insulin secretion. Notably, core components of the stimulus-secretion-coupling mechanism (e.g., *Abcc8*, *Kcnj11*, and *Cacna1c*) and genes encoding proteins important for vesicle docking (e.g., *Pclo* and *Noc2*) were normally expressed in Nkx6.1-deficient islets (Figure 3G).

To directly test whether the observed changes in gene expression affect insulin secretion at a functional level, we performed in vitro glucose-stimulated insulin secretion (GSIS) assays on isolated islets from *Nkx6.1*$^{\Delta adult\beta}$ and control mice. To account for the decreased insulin content of Nkx6.1-deficient beta cells, we calculated insulin secretion as a percentage of total islet insulin content. Islets from *Nkx6.1*$^{\Delta adult\beta}$ mice secreted less of their total insulin than the control islets under conditions of basal (2.7 mM) and high (16.7 mM) glucose concentrations (Figure 3J), showing that insulin secretion is impaired after *Nkx6.1* deletion. However, stimulation of secretion by glucose appeared to be unaffected by *Nkx6.1* deletion, as there was a similar increase in insulin secretion in *Nkx6.1*$^{\Delta adult\beta}$ and control islets under both low- and high-glucose conditions (3.75-fold increase between 2.7 mM and 16.7 mM glucose in *Nkx6.1*$^{\Delta adult\beta}$ islets versus a 3.06-fold increase in control islets). The insulin secretory pattern of *Nkx6.1*$^{\Delta adult\beta}$ islets is highly similar to the pattern observed in Glut2-deficient islets (Guillam et al., 2000), suggesting that loss of Glut2 in *Nkx6.1*$^{\Delta adult\beta}$ beta cells makes a major contribution to the insulin secretory defect. Notably, additional defects downstream of K_{ATP} channel-mediated membrane depolarization also appear to exist, as insulin secretion in Nkx6.1-deficient islets was also reduced in response to membrane depolarization and calcium influx (30 mM KCl and 2 μM Bay K8644, respectively; Figure 3J). Together, these results imply that impaired insulin secretion is a major contributor to the diabetic phenotype of *Nkx6.1*$^{\Delta adult\beta}$ mice.

Decreased Beta Cell Proliferation in *Nkx6.1*$^{\Delta adult\beta}$ Mice

It has been suggested that glycolytic flux and ATP production serve as a trigger for beta cell replication (Porat et al., 2011). Specifically, glucose metabolism is thought to control beta cell proliferation by regulating expression of *Cyclin D2* (*Ccnd2*) (Salpeter et al., 2010, 2011), which is a critical regulator of beta cell mass in mice (Georgia and Bhushan, 2004; Kushner et al., 2005). Since Nkx6.1-deficient beta cells have defects in energy production, we examined whether *Nkx6.1* deletion affects *Ccnd2* messenger RNA (mRNA) levels. We found that *Ccnd2* mRNA levels were indeed decreased in *Nkx6.1*$^{\Delta adult\beta}$ islets (Table S1; Figure 4A). Strikingly, *Nkx6.1* inactivation specifically affected *Ccnd2*, whereas the mRNA levels of other *cyclins* were unaffected (Table S1; Figure 4A). Immunofluorescence staining (Figures 4B–4C′) and western blot analysis (Figure 4D) further demonstrated significantly reduced Cyclin D2 protein levels in beta cells of *Nkx6.1*$^{\Delta adult\beta}$ mice. Similar to the phenotype of *Ccnd2* null mutant mice (Georgia and Bhushan, 2004; Kushner et al., 2005), Nkx6.1-deficient beta cells exhibited a reduction in the number of beta cells expressing the proliferation marker Ki67 (Figure 4E), showing that beta cell proliferation is impaired after *Nkx6.1* inactivation. Notably, Nkx6.1

(H) Pancreatic insulin content normalized to protein concentration is reduced in *Nkx6.1*$^{\Delta adult\beta}$ mice (n = 6).

(I and J) Immunofluorescence staining reveals almost complete absence of Nkx6.1 and reduced insulin expression in *Nkx6.1*$^{\Delta adult\beta}$ mice at 7 weeks. The scale bar represents 20 μm. Ins, insulin. Data are shown as mean ± SEM. *p < 0.05, **p < 0.01, ***p < 0.001.

See also Figures S1 and S2.

A

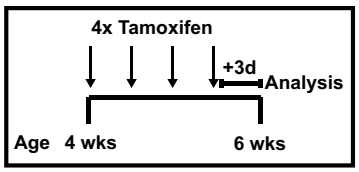

B

Gene ontology of significantly regulated biological processes

Category	Bonferonni P-Value	Gene Symbol
Ion transport	4.54E-09	*Ptger3, Kcnj13, Mcoln3, Trpm5, Slc5a10, Kcnf1, Kcnj5, Slc26a1, Kcnj12, Mfi2, Kcnmb4, Slc4a7, Scnn1a, Kcns3, Adora1, Slc22a2, Atp4a, Cnnm1, Trpm1, Scn3a, Kcnq1**, Slc30a8***
Regulation of secretion	4.44E-08	*Sytl4*, Maob, Cartpt, Adora1, Ucn3*, Kcnq1**, Prkca, Vegfc, Rbp4, Hadh, Cadps2, Chrna4, Adora3, Aacs, Syt9, Niacr1, Agt, Snca, Glul, Snap23*
Oxidation reduction	9.67E-03	*Cybrd1, Cyp4f39, Nox4*, Aldh1a3*, Gpx3*, Maob, Pam, Ero1lb*, Moxd1, Bckdhb, Aldh1l2, Kdm2b, Hsd17b13, Slc1a3, Fmo1, Aass, Dhrs4, Adh1, Egln3, Steap1*
Insulin secretion	1.09E-02	*Sytl4*, Cartpt, Ucn3*, Kcnq1**, Hadh, Slc30a8**, Gpr119, Aacs, Syt9, Glul, Fkbp1b, Rfx6*, Inhbb, Oit1, Glp1r*, Nkx6.1, Oxct1, Adra2a, Irs1**
Hexose biosynthesis	3.48E-02	*Aldob, Rbp4, Pcx*, G6pc2*, Gnpda1, Pck1, Fbp2, Fpgt*

* = Known metabolic function in mice, ** = Associated with type 2 diabetes in GWA studies

C

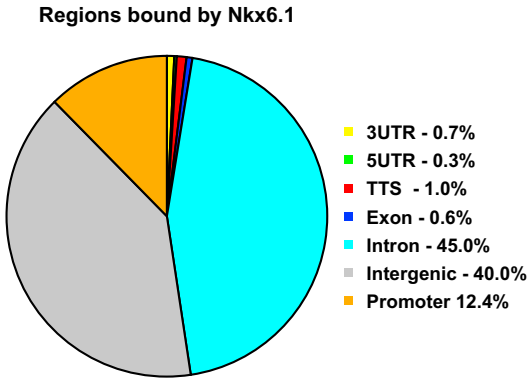

D

E

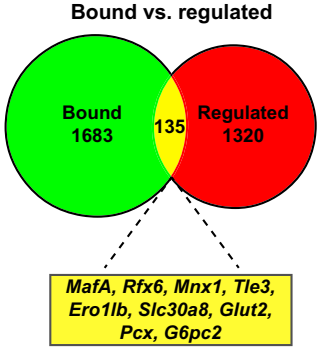

F

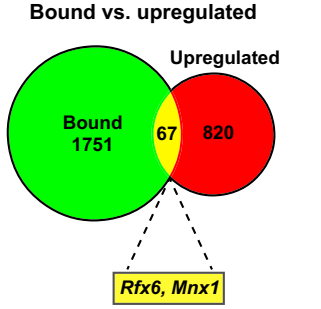

G

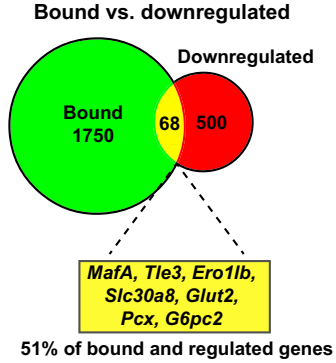

Figure 2. Nkx6.1 Regulates Important Beta Cell Genes

(A) Schematic of experimental design for microarray analysis.

(B) GO analysis of differentially expressed genes as identified by cDNA microarray analysis of *Nkx6.1*$^{\Delta adult\beta}$ and control islets.

(C) Distribution of Nkx6.1 binding peaks from ChIP-seq analysis within the genome.

(D) De novo motif analysis of Nkx6.1 binding peaks identifies a consensus Nkx6.1 binding motif.

(E) Venn diagram of genes bound and regulated by Nkx6.1 in mature islets.

(F and G) Analysis of Nkx6.1-occupied genes reveals Nkx6.1 target genes that are up- and down-regulated after *Nkx6.1* deletion. Yellow boxes represent Nkx6.1-bound and -regulated genes with known function in beta cells. TTS, transcription termination site.

See also Figure S3 and Tables S1, S2, and S3.

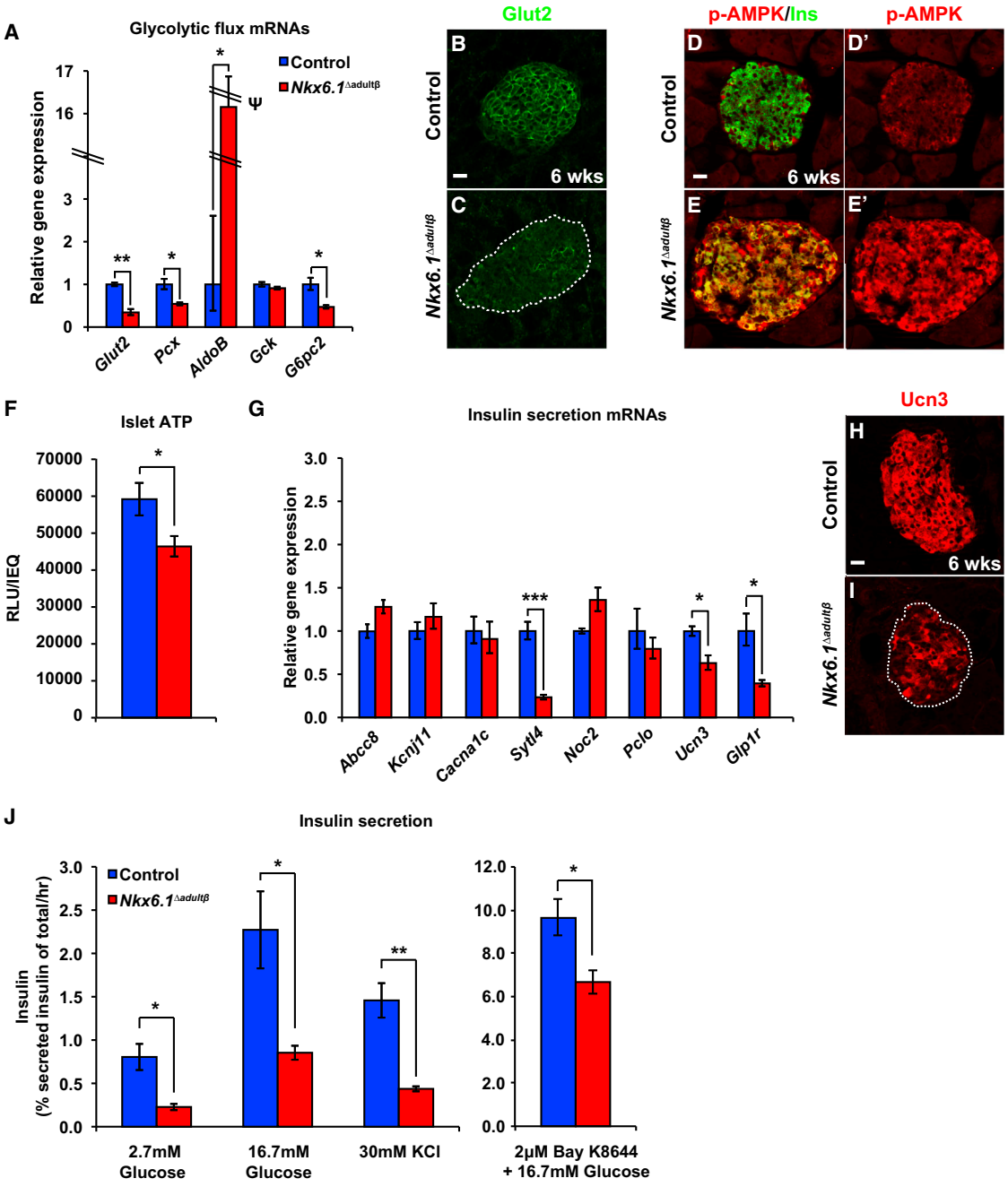

Figure 3. Islets from *Nkx6.1*$^{\Delta adult\beta}$ Mice Exhibit Reduced Insulin Secretion In Vitro

(A) qRT-PCR analysis of islets from *Nkx6.1*$^{\Delta adult\beta}$ and control mice at 6 weeks for genes involved in glycolytic flux (n = 3).

(B–E') Immunofluorescence staining of pancreata from *Nkx6.1*$^{\Delta adult\beta}$ and control mice at 6 weeks.

(F) ATP measurement in islets from *Nkx6.1*$^{\Delta adult\beta}$ and control mice at 6 weeks (n = 8).

(G) qRT-PCR analysis of islets from *Nkx6.1*$^{\Delta adult\beta}$ and control mice at 6 weeks for genes involved in insulin secretion (n = 3).

(H and I) Immunofluorescence staining for Ucn3 in *Nkx6.1*$^{\Delta adult\beta}$ and control pancreata at 6 weeks.

(J) Static incubation of islets from *Nkx6.1*$^{\Delta adult\beta}$ and control mice with 2.7 mM glucose, 16.7 mM glucose, 30 mM KCl, or 2 μM Bay K8644 for 1 hr reveals that the islets from *Nkx6.1*$^{\Delta adult\beta}$ mice secrete less of their total insulin content per hour than the control islets (n = 6). The scale bar represents 20 μm. Dashed lines in (C) and (H) represent islet area. Ins, insulin; p-AMPK, phospho-AMP kinase. Data are shown as mean ± SEM; Ψ = 16.27 with an SEM of ± 2.93. Slashes in A = change in y axis scale. *p < 0.05, **p < 0.01, ***p < 0.001.

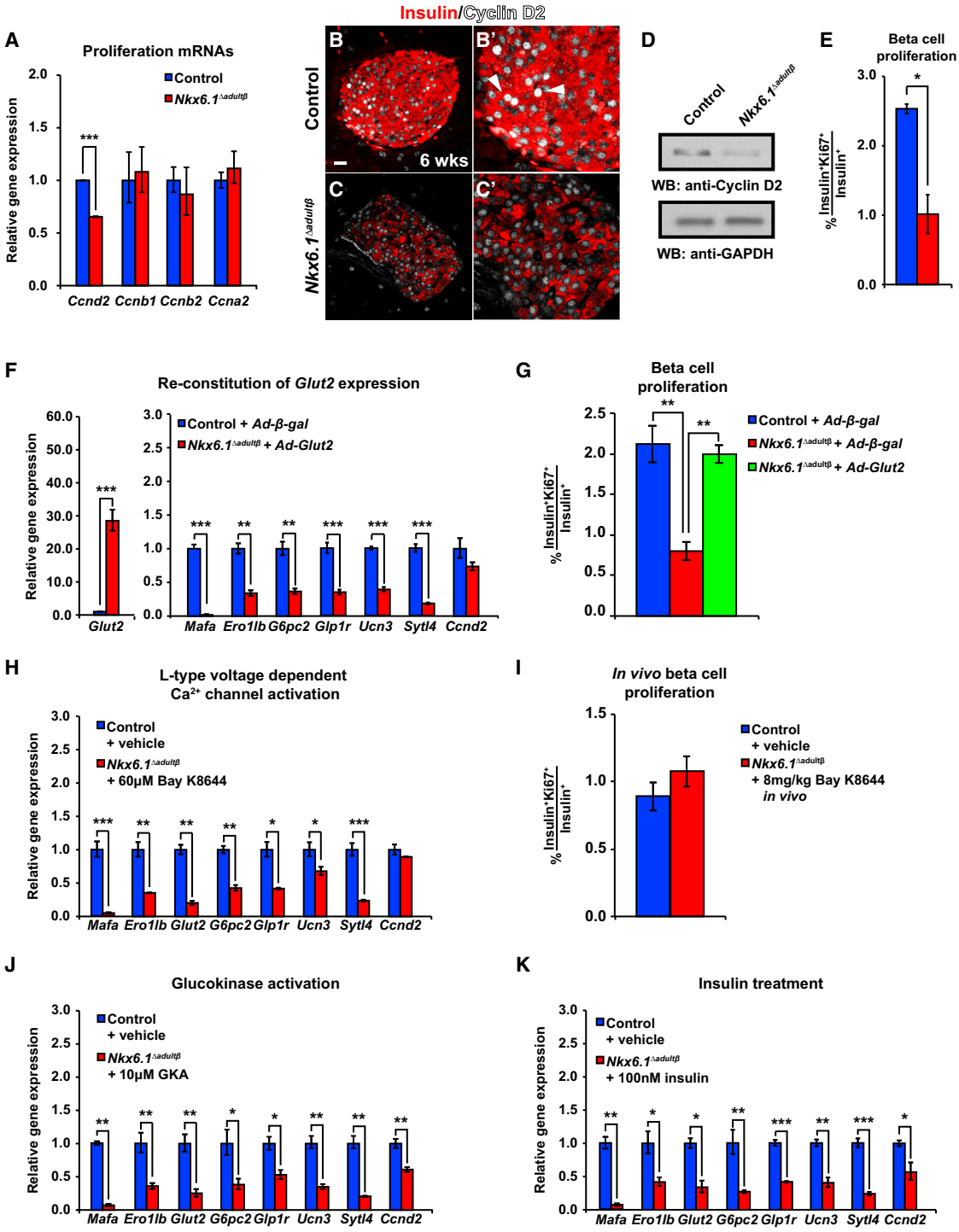

Figure 4. Nkx6.1 Maintains Cyclin D2 Expression and Beta Cell Proliferative Capacity through the Regulation of Glucose Uptake

(A) qRT-PCR analysis of islets shows a decrease in *Ccnd2* expression in *Nkx6.1*$^{\Delta adult\beta}$ compared with control mice at 6 weeks (n = 3).

(B–C') Immunofluorescence staining for insulin and Cyclin D2 shows a decrease in Cyclin D2 expression in beta cells of *Nkx6.1*$^{\Delta adult\beta}$ mice at 6 weeks. (B') and (C') are higher-magnification images of (B) and (C), respectively. White arrowheads point to Cyclin D2^{high} cells.

(D) Immunoblot analysis of whole-cell islet lysates confirms reduced Cyclin D2 expression in *Nkx6.1*$^{\Delta adult\beta}$ mice.

(E) Quantification of the percentage of insulin^{+} cells expressing Ki67 shows decreased beta cell proliferation in *Nkx6.1*$^{\Delta adult\beta}$ mice at 6 weeks (n = 3).

(F) qRT-PCR analysis of genes with decreased expression in islets from *Nkx6.1*$^{\Delta adult\beta}$ mice after adenoviral infection of *Nkx6.1*$^{\Delta adult\beta}$ islets with *Ad-CMV-Glut2* (*Ad-Glut2*) and control islets with *Ad-CMV-β-gal* (*Ad-β-gal*) (n = 3). *Ad-Glut2* restores *Ccnd2* expression to levels observed in control islets infected with *Ad-β-gal*.

(legend continued on next page)

did not occupy *Ccnd2* regulatory sequences (Table S2), suggesting that the regulation of *Ccnd2* by Nkx6.1 could be indirect.

Restoring Glucose Import Reinstates *Ccnd2* Expression in *Nkx6.1*$^{\Delta adult\beta}$ Islets

To explore whether limited glucose uptake capacity due to loss of Glut2 could be the main cause of reduced *Ccnd2* expression in Nkx6.1-deficient islets, we investigated whether restoring Glut2-mediated glucose import could increase *Ccnd2* levels after *Nkx6.1* inactivation. To examine this, we reconstituted *Glut2* expression in *Nkx6.1*$^{\Delta adult\beta}$ islets using an adenovirus containing *Glut2* complementary DNA (cDNA; *Ad-Glut2*), which resulted in a 25-fold increase in *Glut2* mRNA levels compared with *Ad-β-gal*-treated control islets, and restored Glut2 protein expression (Figures 4F and S4). Glut2 reconstitution increased *Ccnd2* expression to the levels of the control islets, whereas expression of other Nkx6.1-regulated genes remained significantly reduced (Figure 4F). Glut2 reconstitution in *Nkx6.1*$^{\Delta adult\beta}$ islets also restored the number of insulin$^+$ cells expressing Ki67 to control values (Figure 4G), indicating that Glut2 reexpression rescues the proliferation defect. These findings demonstrate that *Ccnd2* expression does not depend on direct transcriptional input from Nkx6.1, and that Nkx6.1 controls *Ccnd2* and beta cell proliferation indirectly by regulating glucose import.

Consistent with the notion that glycolytic flux regulates *Ccnd2* expression via the stimulus-secretion-coupling pathway (Salpeter et al., 2010, 2011), increasing calcium influx by treating islets with the L-type-dependent calcium channel opener Bay K8644 similarly restored *Ccnd2* expression in *Nkx6.1*$^{\Delta adult\beta}$ islets (Figure 4H). Significantly, Bay K8644 administration to mice increased the number of insulin$^+$ cells expressing Ki67 to control values (Figure 4I), providing in vivo evidence that beta cell proliferation can be rescued by stimulating calcium influx. In contrast, culture of Nkx6.1-deficient islets in the presence of an activator for the rate-limiting enzyme of glycolysis, glucokinase, or the beta cell mitogen, insulin (Paris et al., 2003), failed to restore *Ccnd2* expression (Figures 4J and 4K; also compare with Figure 4A). These findings illustrate that the proliferative capacity of beta cells is coupled to glucose metabolism and that Nkx6.1 controls this process by regulating *Glut2* expression. Because beta cells have a low turnover rate in adult mice (Teta et al., 2005), the observed reduction in beta cell proliferation did not result in decreased beta cell mass in our acute *Nkx6.1* deletion model (Figures S2G and S2H). However, the decreased proliferative capacity could become metabolically relevant when beta cells need to undergo adaptive expansion under conditions of increased insulin demand.

Nkx6.1$^{\Delta adult\beta}$ Mice Have Posttranscriptional Defects in Insulin Biosynthesis

Our gene expression and ChIP-seq analysis revealed that Nkx6.1 also controlled genes required for insulin biosynthesis, which could explain the reduction in pancreatic insulin levels in *Nkx6.1*$^{\Delta adult\beta}$ mice. Most notably, expression of the T2D-associated zinc transporter *Slc30a8*, the oxidoreductase *Ero1lb*, and the proinsulin-to-insulin convertase *Pcsk1* (PC1) was severely reduced in Nkx6.1-deficient beta cells (Table S1; Figures 5A–5E). These proteins have established roles in insulin processing and/or maturation of insulin secretory vesicles (Bellomo et al., 2011; Zhu et al., 2002; Zito et al., 2010), implying a role for Nkx6.1 in multiple aspects of the insulin biosynthesis pathway. Notably, the finding that *Ins1* and *Ins2* mRNA levels were not significantly changed (Table S1; Figure 5F) suggests that reduced insulin production in *Nkx6.1*$^{\Delta adult\beta}$ mice is mainly caused by posttranscriptional defects in insulin biosynthesis. To further define which steps in insulin biosynthesis are affected by *Nkx6.1* inactivation, we measured pancreatic proinsulin content and calculated the insulin-to-proinsulin ratio in *Nkx6.1*$^{\Delta adult\beta}$ islets. Compared with control mice, pancreatic proinsulin levels and the ratio of insulin to proinsulin were significantly reduced in *Nkx6.1*$^{\Delta adult\beta}$ mice (Figures 5G and 5H). Although the defect in proinsulin-to-insulin processing was expected based on the observed decrease in *Slc30a8*, *Ero1lb*, and *Pcsk1* expression, it is less clear why loss of Nkx6.1 impairs proinsulin biosynthesis.

Because glucose is a direct stimulator of proinsulin translation (Wicksteed et al., 2003), we examined whether decreased Glut2 expression in *Nkx6.1*$^{\Delta adult\beta}$ mice limits the intracellular availability of glucose and in turn reduces proinsulin production. However, restoring *Glut2* expression in *Nkx6.1*$^{\Delta adult\beta}$-dispersed islets had no effect on proinsulin or insulin levels (Figures S5A and S5B), suggesting that reduced expression of insulin biosynthetic enzymes, rather than glucose import, limits proinsulin synthesis in *Nkx6.1*$^{\Delta adult\beta}$ mice.

To determine whether the defect in insulin biosynthesis affects the formation of insulin secretory vesicles, we examined secretory vesicle numbers and morphology in beta cells from *Nkx6.1*$^{\Delta adult\beta}$ and control mice. According to the guidelines established by Pictet et al. (1972), secretory vesicles were considered immature if they had a homogeneous light gray appearance similar to the electron density of the cytoplasm, or mature if the vesicles contained an electron-dense granule darker than the density of the cytoplasm. Transmission electron microscopy (TEM) showed that the overall number of secretory granules was unchanged (Figures 5I–5K), suggesting that loss of Nkx6.1 does not affect vesicle formation or stability. In accordance with the observed defect in insulin biosynthesis, our examination of vesicle morphology revealed a smaller overall

(G) Quantification of the percentage of insulin$^+$ cells expressing Ki67 after infection of *Nkx6.1*$^{\Delta adult\beta}$ and control islets with *Ad-Glut2* or *Ad-β-gal* shows that *Ad-Glut2* restores the number of Ki67$^+$ beta cells in *Nkx6.1*$^{\Delta adult\beta}$ islets to control values (n = 3).
(H) qRT-PCR analysis after a 3 hr treatment of *Nkx6.1*$^{\Delta adult\beta}$ islets with the calcium channel activator Bay K8644 and control islets treated with vehicle (n = 3).
(I) Quantification of the percentage of insulin$^+$ cells expressing Ki67 after injection of *Nkx6.1*$^{\Delta adult\beta}$ mice with 8 mg/kg Bay K8644 or control mice injected with vehicle (n = 3). Stimulation of calcium influx restores *Ccnd2* expression and beta cell proliferation in *Nkx6.1*$^{\Delta adult\beta}$ mice.
(J and K) qRT-PCR analysis of islets from *Nkx6.1*$^{\Delta adult\beta}$ mice treated with 10 μM GKA (J) or 100 nM insulin (K) for 3 hr and islets from control mice treated with vehicle (n = 3). The scale bar represents 20 μm. Data are shown as mean ± SEM. *p < 0.05, **p < 0.01, ***p < 0.001.
See also Figure S4.

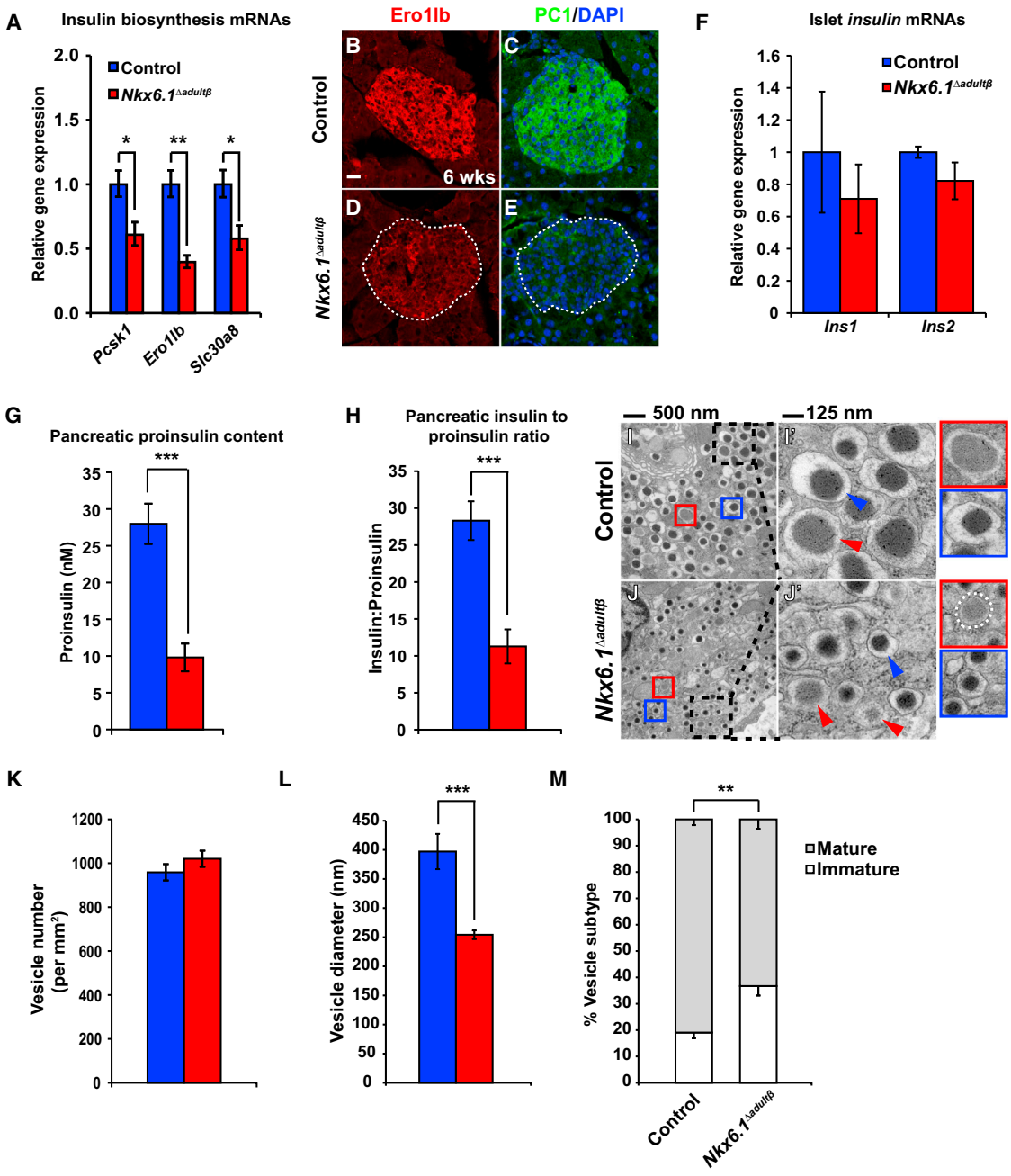

Figure 5. *Nkx6.1* Is Necessary for Insulin Biosynthesis

(A) qRT-PCR analysis of islets reveals reduced expression of genes involved in insulin biosynthesis in *Nkx6.1*$^{\Delta adult\beta}$ compared with control mice at 6 weeks (n = 3).

(B–E) Immunofluorescence staining of pancreata from *Nkx6.1*$^{\Delta adult\beta}$ and control mice at 6 weeks. Dashed lines represent islet area.

(F) qRT-PCR analysis of *Nkx6.1*$^{\Delta adult\beta}$ and control islets from mice at 6 weeks shows no significant difference in *Ins1* or *Ins2* expression (n = 3).

(G) Proinsulin content normalized to the protein concentration of whole pancreatic lysates (n = 6).

(H) The pancreatic insulin-to-proinsulin ratio is reduced in *Nkx6.1*$^{\Delta adult\beta}$ mice (n = 6).

(I and J) TEM of pancreatic sections reveals smaller vesicle size and an increase in immature vesicles (red arrowheads) in *Nkx6.1*$^{\Delta adult\beta}$ compared with control mice. Dashed boxes indicate area of magnification in (I') and (J'). Blue arrowheads point to vesicles containing mature insulin-dense core granules. Insets framed in red show a representation of a typical immature vesicle, and insets framed in blue show a typical mature vesicle.

(K–M) Quantification of vesicle numbers (K), vesicle diameter (L), and the percentage of mature and immature vesicles (M) in *Nkx6.1*$^{\Delta adult\beta}$ and control mice (n = 10). In (G)–(M), mice were analyzed at 7 weeks. PC1, prohormone convertase 1/3. Data are shown as mean ± SEM for (A) and (F)–(H), and ±SD for (K)–(M). *p < 0.05, **p < 0.01, ***p < 0.001.

See also Figure S5.

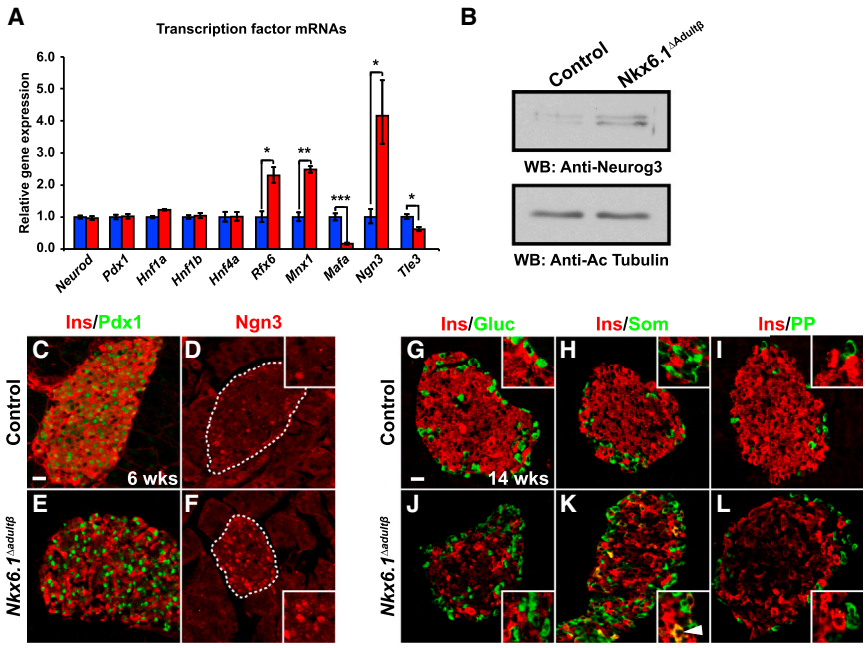

Figure 6. Increased Expression of the Progenitor Marker Ngn3 in Nkx6.1-Deficient Beta Cells

(A and B) qRT-PCR (A) and western blot analysis (B) of islets from *Nkx6.1*$^{\Delta adult\beta}$ and control mice at 6 weeks for multiple transcription factor genes (A) or Ngn3 (B); n = 3.

(C–L) Immunofluorescence staining of pancreata from *Nkx6.1*$^{\Delta adult\beta}$ and control mice at 6 weeks (C–F) and 14 weeks (G–L). Dashed lines represent islet area. Insets are magnifications of selected areas. Arrowhead in (K) points to a cell coexpressing insulin (Ins) and somatostatin (Som). The scale bar represents 20 μm. Gluc, glucagon; PP, pancreatic polypeptide. Data are shown as mean ± SEM. *p < 0.05, **p < 0.01, ***p < 0.001.

vesicle size in beta cells of *Nkx6.1*$^{\Delta adult\beta}$ mice (Figures 5I′, 5J′, and 5L). Reduced vesicle size was similarly observed in the *MODY* (*Ins2*^{Akita}) mouse model of impaired insulin biosynthesis (Wang et al., 1999). In addition to their reduced size, secretory granules in beta cells of *Nkx6.1*$^{\Delta adult\beta}$ mice exhibited a smaller halo around the dense core of mature insulin (Figures 5I′ and 5J′, blue arrowheads), a feature that reflects reduced processing of proinsulin to insulin (Orci et al., 1984). Moreover, the proportion of immature vesicles was significantly increased in Nkx6.1-deficient beta cells (Figure 5M), representing another feature of impaired insulin processing. These findings demonstrate that changes in the expression of insulin biosynthesis-associated genes after *Nkx6.1* deletion manifest as defects in insulin processing and mature insulin secretory vesicle formation. Given previous evidence that deletion of *Ero1lb* and *Slc30a8* in mice perturbs glucose homeostasis (Nicolson et al., 2009; Zito et al., 2010), these defects in insulin biosynthesis together with the impaired insulin secretory response are likely the predominant cause of diabetes in *Nkx6.1*$^{\Delta adult\beta}$ mice.

Nkx6.1 Inactivation Destabilizes Beta Cell Identity

In T2D mouse models of metabolic stress, reduced beta cell insulin production is associated with a decrease in *Nkx6.1*, *Pdx1*, and *NeuroD* expression, as well as increased expression of the pancreatic progenitor cell *marker Ngn3* and the pluripotency markers *Oct4*, *Nanog*, and *L-Myc* (Talchai et al., 2012). Because a subset of metabolically stressed beta cells eventually adopt other endocrine fates, it has been proposed that beta cell dedifferentiation followed by conversion into other endocrine cell types could cause beta cell failure in T2D (Talchai et al., 2012). Although *Nkx6.1* deletion did not affect the expression of *Pdx1*, *NeuroD*, or pluripotency markers (Table S1; Figures 6A, 6C, and 6E), we observed robust induction of Ngn3 expression in beta cells similar to what has been observed in models of metabolic stress (Table S1; Figures 6A, 6B, 6D, and 6F). To investigate whether the upregulation of Ngn3 is associated with destabilization of beta cell identity, we examined pancreata from *Nkx6.1*$^{\Delta adult\beta}$ mice at 14 weeks of age (8 weeks after *Nkx6.1* deletion) for coexpression of insulin with other pancreatic hormones. We did not observe coexpression of insulin with glucagon or pancreatic polypeptide in *Nkx6.1*$^{\Delta adult\beta}$ or control islets, but found a significant number of insulin^{+} cells coexpressing somatostatin in *Nkx6.1*$^{\Delta adult\beta}$ mice (Figures 6G–6L). This finding is consistent with our previous observation of a beta-to-delta cell fate switch after *Nkx6.1* ablation in embryonic beta cells (Schaffer et al., 2013) and suggests that, although it does not happen immediately, *Nkx6.1* inactivation in adult beta cells causes beta cells to adopt a delta cell identity over time. In conjunction with our previous findings, these data strongly suggest that loss of *Nkx6.1* in adult mice destabilizes beta cell identity, eventually leading to fate conversion of beta into delta cells.

Together, our analysis demonstrates that Nkx6.1 is a critical regulator of insulin biosynthesis and secretion, as well as proliferative capacity and cell identity in adult beta cells. The severe beta cell defects observed after *Nkx6.1* inactivation suggest that restoring Nkx6.1 levels could be a therapeutic strategy in T2D.

DISCUSSION

It is widely recognized that beta cell dysfunction, specifically the inability of beta cells to properly secrete insulin in response to high blood glucose levels, is among the earliest clinical features during progression to T2D (Ferrannini, 2010). The ability to sense glucose levels and to couple this information to an insulin secretory response is bestowed upon beta cells by specialized transporters and enzymes. Although the mechanisms that underlie glucose-mediated insulin secretion are fairly well understood, it has remained unclear which transcriptional regulators initiate and maintain the expression of genes that enable beta cells to perform their highly specialized function. In this study, we show that the transcription factor Nkx6.1 is a master regulator

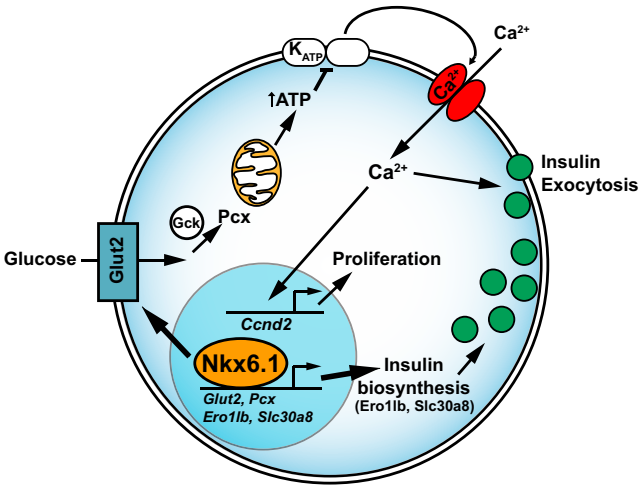

Figure 7. Nkx6.1 Function in Adult Beta Cells

Nkx6.1 directly regulates transcription of genes encoding proteins involved in glucose uptake and metabolism (Glut2 and Pcx) and insulin biosynthesis (Ero1lb and Slc30a8). Reduced expression of these Nkx6.1 target genes affects beta cell function in three ways: First, decreased glucose uptake and metabolism diminishes ATP production, leading to impaired insulin secretion via the stimulus-secretion coupling pathway. Second, by enabling glucose uptake through Glut2 regulation, Nkx6.1 indirectly controls beta cell proliferative capacity. In the absence of Nkx6.1, expression of *Ccnd2*, which encodes the critical beta cell mitogen Cyclin D2, is reduced and beta cell proliferation is decreased. Reconstituting Glut2 expression in Nkx6.1-deficient beta cells restores *Ccnd2* levels and beta cell proliferation. Third, insulin biosynthesis is severely impaired, leading to reduced production of mature insulin and an overabundance of immature secretory vesicles. Gck, glucokinase; Glut2, glucose transporter 2; K_{ATP}, ATP-sensitive potassium channel; Pcx, pyruvate carboxylase.

of genes that define the functional beta cell state, a role that is consistent with its exclusive expression in beta cells of the adult pancreas.

We show that conditional inactivation of *Nkx6.1* in beta cells of adult mice results in overt diabetes within days of *Nkx6.1* ablation. Loss of Nkx6.1 activity had an immediate and dramatic impact on the expression of genes that give beta cells their unique ability to synthesize and release insulin in a regulated fashion. We found that genes involved in insulin biosynthesis (*Slc30a8* and *Ero1lb*), glucose import (*Glut2*), and glucose metabolism (*Pcx*) are direct transcriptional target genes of Nkx6.1. In addition, *Nkx6.1* ablation indirectly affected the expression of numerous genes that are important for beta cell function and, interestingly, also beta cell proliferation (Figure 7). The finding that islet *Ccnd2* levels and beta cell proliferation were decreased in *Nkx6.1* conditional mutant mice was somewhat surprising, as several studies have shown that hyperglycemia has a stimulatory effect on beta cell *Ccnd2* expression and self-renewal (Alonso et al., 2007; Bonner-Weir et al., 1989; Salpeter et al., 2011). We found that reduced availability of the beta cell mitogen insulin (Paris et al., 2003) made no apparent contribution to the reduced proliferative capacity of beta cells after *Nkx6.1* ablation. Instead, our results suggest that the proliferative capacity of Nkx6.1-deficient beta cells is limited by the reduced intracellular availability of glucose due to loss of *Glut2* expression (Figure 7). These findings demonstrate an intricate link between the beta cell's ability to import glucose and its proliferative capacity, which lends further support to the emerging concept that glucose metabolism plays a critical role in the regulation of beta cell proliferation (Porat et al., 2011; Salpeter et al., 2010, 2011). Combined with the finding that Nkx6.1 levels are reduced in T2D models of metabolic stress (Talchai et al., 2012), our work suggests that Nkx6.1 acts as a metabolic sensor that modulates both insulin secretion and proliferative capacity in response to metabolic stress. By preventing the proliferation of beta cells that have lost glucose responsiveness, the cell-autonomous coupling of glucose import to beta cell proliferation might provide an inherent selection mechanism for healthy beta cells.

Our study also reconciles previously reported, seemingly contradictory findings about the role of Nkx6.1 in beta cell proliferation. We recently reported that transgenic overexpression of Nkx6.1 in beta cells of adult mice in vivo had no positive effect on beta cell proliferation or beta cell mass (Schaffer et al., 2011). By contrast, virus-mediated expression of Nkx6.1 in cultured islets had proproliferative activity (Schisler et al., 2008). A possible explanation for this apparent contradiction is that in vitro culture of islets compromises Nkx6.1 expression levels. It is known that once they are removed from their niche and put into culture, beta cells quickly lose Glut2 expression and cease to proliferate (Weinberg et al., 2007), indicating that expression of upstream Glut2 regulators, including Nkx6.1, could also be compromised. Thus, the observed proproliferative effect of Nkx6.1 in vitro may be explained by virally expressed *Nkx6.1* restoring reduced Nkx6.1 levels and, in turn, also Glut2 and Ccnd2 levels in cultured islets. By contrast, increasing Nkx6.1 levels above normal in healthy beta cells in vivo appears to have no further stimulatory effect on glucose import and beta cell proliferation.

After *Nkx6.1* deletion, we observed an extremely rapid decline in beta cell insulin content. The loss of insulin was not associated with beta cell death, revealing a striking similarity between Nkx6.1-deficient beta cells and "empty" beta cells observed in mouse models of T2D (Talchai et al., 2012). Furthermore, as reported under conditions of metabolic stress (Talchai et al., 2012), we found that reduced *Nkx6.1* expression was also accompanied by derepression of the endocrine progenitor cell marker Ngn3. Based on the observation that beta cells undergo fate conversion into non-beta endocrine cell types in T2D models (Talchai et al., 2012), the loss of beta cell features and gain of Ngn3 expression has been proposed to render beta cells plastic and more prone to changing their identity.

Consistent with this notion, we observed that a subset of Nkx6.1-deficient beta cells ectopically expressed somatostatin 8 weeks after *Nkx6.1* deletion. Previously, we showed with lineage tracing studies that *Nkx6.1* deletion in embryonic beta cells leads to a rapid beta-to-delta cell fate switch (Schaffer et al., 2013). However, conversion of beta cells into other non-beta endocrine cell types was not observed after *Nkx6.1* inactivation in embryonic beta cells. Similarly, after *Nkx6.1* deletion in adult beta cells, we observed coexpression of insulin exclusively with somatostatin and no other pancreatic hormones. Thus, loss of Nkx6.1 leads to selective derepression of delta cell genes in both embryonic and adult beta cells. However, fate conversion

is more complete and occurs more rapidly when *Nkx6.1* is inactivated in immature beta cells. Therefore, a sequential loss of beta cell traits preceding the adoption of alternative endocrine cell fates seen after adult *Nkx6.1* inactivation closely mirrors the gradual loss of functional beta cell mass observed in T2D models (Talchai et al., 2012).

Our study provides support for an evolving concept that transcription factors, such as Nkx6.1 and FoxO1 (Talchai et al., 2012), are critical for maintaining beta cells in their differentiated state. A key question that requires further exploration is whether a destabilized beta cell state is observed in humans and possibly contributes to the pathogenesis of T2D. The observation that NKX6.1 expression is decreased in beta cells from humans with T2D (Guo et al., 2013) suggests that findings in rodent models might indeed be relevant to human disease. Future studies will need to explore which aspects of the rodent phenotype are also found in humans and how loss of beta cell features relates to disease progression. Such knowledge could identify a window for therapeutic intervention during which the functional beta cell state could be restored before beta cells convert into other endocrine cell types.

EXPERIMENTAL PROCEDURES

Mouse Strains

The following mouse strains were utilized in this study: *Pdx1CreER^{TM}* (Gu et al., 2002), *Nkx6.1$^{+/-}$* (Sander et al., 2000), and *Nkx6.1^{flox}* (Schaffer et al., 2013). All animals carrying the *Nkx6.1^{flox}* allele were maintained on a mixed 129Sv/C57Bl6/J genetic background. Unless otherwise stated in the text, male mice were used for the experiments. Tamoxifen (Sigma) was dissolved in corn oil at 20 mg/ml, and 2 mg was injected subcutaneously four times over a 2-week period. All animal experiments were approved by the Institutional Animal Care and Use Committees of the University of California, San Diego.

Tissue Preparation and Immunohistochemistry

Tissue preparation, immunofluorescence staining, TUNEL assays, and morphometry were performed as previously described (Schaffer et al., 2010, 2013). A description of the antibodies used (Tables S4 and S5) and detailed methods are provided in the Extended Experimental Procedures.

Microscopy and Image Analysis

All immunofluorescent images were acquired using a Zeiss AxioOberver.Z1 microscope (Carl Zeiss) with the Zeiss ApoTome module and processed in Zeiss AxioVision Release 4.8 and Adobe Photoshop CS5.1. Only brightness and contrast was adjusted in images in accordance with the *Journal of Cell Biology* figure manipulation guidelines.

Glucose Tolerance Tests, GSIS Assays, and Insulin and Proinsulin Measurements

Glucose tolerance tests, GSIS assays, and insulin measurements were performed as previously described (Schaffer et al., 2011). Proinsulin measurements were performed on whole pancreatic lysates using a mouse proinsulin ELISA (ALPCO). Details are described in the Extended Experimental Procedures.

Islet Isolation and Culture

Islet isolations were performed as previously described (Schaffer et al., 2011) with Liberase TL (Roche). For incubation of islets with chemical compounds, RPMI supplemented with 2.7 mM glucose and 1% BSA was used. *Nkx6.1$^{\Delta adult\beta}$* islets were incubated with 100 nM recombinant insulin (Sigma), 60 μM ± Bay K8644 (Sigma), or 10 μM glucokinase activator (GKA; EMD Calbiochem), and control islets were incubated with DMSO (ATCC) for 3 hr. For infection of islets with *Ad-Glut2* and *Ad-β-gal*, the islets were dispersed and plated before infection as described previously (Fiaschi-Taesch et al., 2009). Further details are provided in the Extended Experimental Procedures.

Microarray and qRT-PCR

RNA was isolated from islets obtained from six littermate control and six *Nkx6.1$^{\Delta adult\beta}$* mice. Islets from two mice of identical genotypes were pooled to generate three independent cDNA probes per genotype for array hybridization. Labeled cDNA was hybridized to whole-mouse gene-expression G2519F microarrays (Agilent Technologies). A detailed description of the microarray and qRT-PCR analyses and a list of the primer sequences (Table S6) can be found in the Extended Experimental Procedures.

ChIP-Seq

ChIP was performed as previously described (Schaffer et al., 2013) with rabbit anti-Nkx6.1 antiserum (1:250) on sheared chromatin obtained from ~10,000 islet equivalents (1,000 cells per islet) isolated from C57BL/6J mice. ChIP-seq libraries were prepared according to Illumina's instructions (http://www.illumina.com). Sequencing was performed on an Illumina/Solexa Genome Analyzer II in accordance with the manufacturer's protocols. Data analysis was performed using Hypergeometric Optimization of Motif EnRichment (HOMER) (Heinz et al., 2010). Peak annotation and de novo motif analysis were performed using HOMER, and venn diagrams were generated using BioVenn (Hulsen et al., 2008). See the Extended Experimental Procedures for details.

Statistics

Unless otherwise stated, all values are shown as mean ± SEM; p values were calculated using an unpaired Student's t test in Microsoft Excel, and hypergeometric distribution was determined using R; $p < 0.05$ was considered significant.

ACCESSION NUMBERS

The NCBI GEO (http://www.ncbi.nlm.nih.gov/geo/) accession number for the microarray data set reported in this paper is GSE40470. The GEO accession number for the ChIP-seq data set reported in this paper is GSE40975.

SUPPLEMENTAL INFORMATION

Supplemental Information includes Extended Experimental Procedures, five figures, and six tables and can be found with this article online at http://dx.doi.org/10.1016/j.celrep.2013.08.010.

ACKNOWLEDGMENTS

We are grateful to D. Melton (Harvard University) for *Pdx1-CreER^{TM}* mice, C. Newgard (Duke University) for *Ad-Glut2* and *Ad-β-gal* adenoviruses, and the following colleagues for anti-sera: P. Serup (DanStem) for anti-Nkx6.1, C. Wright (Vanderbilt University) for anti-Pdx1, M. Huising (Salk Institute) for anti-Ucn3, D. Ron (University of Cambridge) for anti-Ero1lb, D. Steiner (University of Chicago) for anti-PC1/3, and C. Kioussi (Oregon State University) for anti-GFP. We thank N. Rosenblatt for mouse husbandry, R. Xie for assistance with ChIP-seq library preparation, the University of California, San Diego, BioGEM Core for microarray experiments, the University of Pennsylvania Functional Genomics Core for ChIP-seq analysis, the University of California, San Diego, Electron Microscopy Core for assistance with sample preparation for electron microscopy, and members of the Sander laboratory for helpful discussions and critical readings of the manuscript. This work was supported by National Institutes of Health grants R01-DK068471 and U01-DK089567 to M.S.

Received: January 21, 2013
Revised: July 11, 2013
Accepted: August 5, 2013
Published: September 12, 2013

REFERENCES

Alonso, L.C., Yokoe, T., Zhang, P., Scott, D.K., Kim, S.K., O'Donnell, C.P., and Garcia-Ocaña, A. (2007). Glucose infusion in mice: a new model to induce beta-cell replication. Diabetes *56*, 1792–1801.

Bellomo, E.A., Meur, G., and Rutter, G.A. (2011). Glucose regulates free cytosolic Zn^{2+} concentration, Slc39 (ZiP), and metallothionein gene expression in primary pancreatic islet β-cells. J. Biol. Chem. *286*, 25778–25789.

Bhinge, A.A., Kim, J., Euskirchen, G.M., Snyder, M., and Iyer, V.R. (2007). Mapping the chromosomal targets of STAT1 by Sequence Tag Analysis of Genomic Enrichment (STAGE). Genome Res. *17*, 910–916.

Bonner-Weir, S., Deery, D., Leahy, J.L., and Weir, G.C. (1989). Compensatory growth of pancreatic beta-cells in adult rats after short-term glucose infusion. Diabetes *38*, 49–53.

Butler, A.E., Janson, J., Bonner-Weir, S., Ritzel, R., Rizza, R.A., and Butler, P.C. (2003). Beta-cell deficit and increased beta-cell apoptosis in humans with type 2 diabetes. Diabetes *52*, 102–110.

Cerasi, E., and Luft, R. (1967). The plasma insulin response to glucose infusion in healthy subjects and in diabetes mellitus. Acta Endocrinol. (Copenh.) *55*, 278–304.

Ferrannini, E. (2010). The stunned beta cell: a brief history. Cell Metab. *11*, 349–352.

Fiaschi-Taesch, N., Bigatel, T.A., Sicari, B., Takane, K.K., Salim, F., Velazquez-Garcia, S., Harb, G., Selk, K., Cozar-Castellano, I., and Stewart, A.F. (2009). Survey of the human pancreatic beta-cell G1/S proteome reveals a potential therapeutic role for cdk-6 and cyclin D1 in enhancing human beta-cell replication and function in vivo. Diabetes *58*, 882–893.

Froguel, P., Vaxillaire, M., Sun, F., Velho, G., Zouali, H., Butel, M.O., Lesage, S., Vionnet, N., Clément, K., Fougerousse, F., et al. (1992). Close linkage of glucokinase locus on chromosome 7p to early-onset non-insulin-dependent diabetes mellitus. Nature *356*, 162–164.

Georgia, S., and Bhushan, A. (2004). Beta cell replication is the primary mechanism for maintaining postnatal beta cell mass. J. Clin. Invest. *114*, 963–968.

Gomi, H., Mizutani, S., Kasai, K., Itohara, S., and Izumi, T. (2005). Granuphilin molecularly docks insulin granules to the fusion machinery. J. Cell Biol. *171*, 99–109.

Gu, G., Dubauskaite, J., and Melton, D.A. (2002). Direct evidence for the pancreatic lineage: NGN3+ cells are islet progenitors and are distinct from duct progenitors. Development *129*, 2447–2457.

Guillam, M.T., Dupraz, P., and Thorens, B. (2000). Glucose uptake, utilization, and signaling in GLUT2-null islets. Diabetes *49*, 1485–1491.

Guo, S., Dai, C., Guo, M., Taylor, B., Harmon, J.S., Sander, M., Robertson, R.P., Powers, A.C., and Stein, R. (2013). Inactivation of specific β cell transcription factors in type 2 diabetes. J. Clin. Invest. Published online July 1, 2013. http://dx.doi.org/10.1172/JCI65390.

Heinz, S., Benner, C., Spann, N., Bertolino, E., Lin, Y.C., Laslo, P., Cheng, J.X., Murre, C., Singh, H., and Glass, C.K. (2010). Simple combinations of lineage-determining transcription factors prime cis-regulatory elements required for macrophage and B cell identities. Mol. Cell *38*, 576–589.

Hosker, J.P., Rudenski, A.S., Burnett, M.A., Matthews, D.R., and Turner, R.C. (1989). Similar reduction of first- and second-phase B-cell responses at three different glucose levels in type II diabetes and the effect of gliclazide therapy. Metabolism *38*, 767–772.

Hulsen, T., de Vlieg, J., and Alkema, W. (2008). BioVenn - a web application for the comparison and visualization of biological lists using area-proportional Venn diagrams. BMC Genomics *9*, 488.

Jonas, J.C., Sharma, A., Hasenkamp, W., Ilkova, H., Patanè, G., Laybutt, R., Bonner-Weir, S., and Weir, G.C. (1999). Chronic hyperglycemia triggers loss of pancreatic beta cell differentiation in an animal model of diabetes. J. Biol. Chem. *274*, 14112–14121.

Jørgensen, M.C., Vestergård Petersen, H., Ericson, J., Madsen, O.D., and Serup, P. (1999). Cloning and DNA-binding properties of the rat pancreatic beta-cell-specific factor Nkx6.1. FEBS Lett. *461*, 287–294.

Kushner, J.A., Ciemerych, M.A., Sicinska, E., Wartschow, L.M., Teta, M., Long, S.Y., Sicinski, P., and White, M.F. (2005). Cyclins D2 and D1 are essential for postnatal pancreatic beta-cell growth. Mol. Cell. Biol. *25*, 3752–3762.

Li, C., Chen, P., Vaughan, J., Lee, K.F., and Vale, W. (2007). Urocortin 3 regulates glucose-stimulated insulin secretion and energy homeostasis. Proc. Natl. Acad. Sci. USA *104*, 4206–4211.

Muoio, D.M., and Newgard, C.B. (2008). Mechanisms of disease: molecular and metabolic mechanisms of insulin resistance and beta-cell failure in type 2 diabetes. Nat. Rev. Mol. Cell Biol. *9*, 193–205.

Nicolson, T.J., Bellomo, E.A., Wijesekara, N., Loder, M.K., Baldwin, J.M., Gyulkhandanyan, A.V., Koshkin, V., Tarasov, A.I., Carzaniga, R., Kronenberger, K., et al. (2009). Insulin storage and glucose homeostasis in mice null for the granule zinc transporter ZnT8 and studies of the type 2 diabetes-associated variants. Diabetes *58*, 2070–2083.

Orci, L., Ravazzola, M., Amherdt, M., Yanaihara, C., Yanaihara, N., Halban, P., Renold, A.E., and Perrelet, A. (1984). Insulin, not C-peptide (proinsulin), is present in crinophagic bodies of the pancreatic B-cell. J. Cell Biol. *98*, 222–228.

Paris, M., Bernard-Kargar, C., Berthault, M.F., Bouwens, L., and Ktorza, A. (2003). Specific and combined effects of insulin and glucose on functional pancreatic beta-cell mass in vivo in adult rats. Endocrinology *144*, 2717–2727.

Pictet, R.L., Clark, W.R., Williams, R.H., and Rutter, W.J. (1972). An ultrastructural analysis of the developing embryonic pancreas. Dev. Biol. *29*, 436–467.

Piston, D.W., Knobel, S.M., Postic, C., Shelton, K.D., and Magnuson, M.A. (1999). Adenovirus-mediated knockout of a conditional glucokinase gene in isolated pancreatic islets reveals an essential role for proximal metabolic coupling events in glucose-stimulated insulin secretion. J. Biol. Chem. *274*, 1000–1004.

Porat, S., Weinberg-Corem, N., Tornovsky-Babaey, S., Schyr-Ben-Haroush, R., Hija, A., Stolovich-Rain, M., Dadon, D., Granot, Z., Ben-Hur, V., White, P., et al. (2011). Control of pancreatic β cell regeneration by glucose metabolism. Cell Metab. *13*, 440–449.

Preitner, F., Ibberson, M., Franklin, I., Binnert, C., Pende, M., Gjinovci, A., Hansotia, T., Drucker, D.J., Wollheim, C., Burcelin, R., and Thorens, B. (2004). Gluco-incretins control insulin secretion at multiple levels as revealed in mice lacking GLP-1 and GIP receptors. J. Clin. Invest. *113*, 635–645.

Robertson, R.P. (2004). Chronic oxidative stress as a central mechanism for glucose toxicity in pancreatic islet beta cells in diabetes. J. Biol. Chem. *279*, 42351–42354.

Salpeter, S.J., Klein, A.M., Huangfu, D., Grimsby, J., and Dor, Y. (2010). Glucose and aging control the quiescence period that follows pancreatic beta cell replication. Development *137*, 3205–3213.

Salpeter, S.J., Klochendler, A., Weinberg-Corem, N., Porat, S., Granot, Z., Shapiro, A.M., Magnuson, M.A., Eden, A., Grimsby, J., Glaser, B., and Dor, Y. (2011). Glucose regulates cyclin D2 expression in quiescent and replicating pancreatic β-cells through glycolysis and calcium channels. Endocrinology *152*, 2589–2598.

Sander, M., Paydar, S., Ericson, J., Briscoe, J., Berber, E., German, M., Jessell, T.M., and Rubenstein, J.L. (2000). Ventral neural patterning by Nkx homeobox genes: Nkx6.1 controls somatic motor neuron and ventral interneuron fates. Genes Dev. *14*, 2134–2139.

Schaffer, A.E., Freude, K.K., Nelson, S.B., and Sander, M. (2010). Nkx6 transcription factors and Ptf1a function as antagonistic lineage determinants in multipotent pancreatic progenitors. Dev. Cell *18*, 1022–1029.

Schaffer, A.E., Yang, A.J., Thorel, F., Herrera, P.L., and Sander, M. (2011). Transgenic overexpression of the transcription factor Nkx6.1 in β-cells of mice does not increase β-cell proliferation, β-cell mass, or improve glucose clearance. Mol. Endocrinol. *25*, 1904–1914.

Schaffer, A.E., Taylor, B.L., Benthuysen, J.R., Liu, J., Thorel, F., Yuan, W., Jiao, Y., Kaestner, K.H., Herrera, P.L., Magnuson, M.A., et al. (2013). Nkx6.1 controls a gene regulatory network required for establishing and maintaining pancreatic Beta cell identity. PLoS Genet. *9*, e1003274.

Schisler, J.C., Jensen, P.B., Taylor, D.G., Becker, T.C., Knop, F.K., Takekawa, S., German, M., Weir, G.C., Lu, D., Mirmira, R.G., and Newgard, C.B. (2005). The Nkx6.1 homeodomain transcription factor suppresses glucagon expression and regulates glucose-stimulated insulin secretion in islet beta cells. Proc. Natl. Acad. Sci. USA *102*, 7297–7302.

Schisler, J.C., Fueger, P.T., Babu, D.A., Hohmeier, H.E., Tessem, J.S., Lu, D., Becker, T.C., Naziruddin, B., Levy, M., Mirmira, R.G., and Newgard, C.B. (2008). Stimulation of human and rat islet beta-cell proliferation with retention of function by the homeodomain transcription factor Nkx6.1. Mol. Cell. Biol. *28*, 3465–3476.

Schnedl, W.J., Ferber, S., Johnson, J.H., and Newgard, C.B. (1994). STZ transport and cytotoxicity. Specific enhancement in GLUT2-expressing cells. Diabetes *43*, 1326–1333.

Supale, S., Li, N., Brun, T., and Maechler, P. (2012). Mitochondrial dysfunction in pancreatic β cells. Trends Endocrinol. Metab. *23*, 477–487.

Talchai, C., Xuan, S., Lin, H.V., Sussel, L., and Accili, D. (2012). Pancreatic β cell dedifferentiation as a mechanism of diabetic β cell failure. Cell *150*, 1223–1234.

Terauchi, Y., Sakura, H., Yasuda, K., Iwamoto, K., Takahashi, N., Ito, K., Kasai, H., Suzuki, H., Ueda, O., Kamada, N., et al. (1995). Pancreatic beta-cell-specific targeted disruption of glucokinase gene. Diabetes mellitus due to defective insulin secretion to glucose. J. Biol. Chem. *270*, 30253–30256.

Teta, M., Long, S.Y., Wartschow, L.M., Rankin, M.M., and Kushner, J.A. (2005). Very slow turnover of beta-cells in aged adult mice. Diabetes *54*, 2557–2567.

Wang, J., Takeuchi, T., Tanaka, S., Kubo, S.K., Kayo, T., Lu, D., Takata, K., Koizumi, A., and Izumi, T. (1999). A mutation in the insulin 2 gene induces diabetes with severe pancreatic beta-cell dysfunction in the Mody mouse. J. Clin. Invest. *103*, 27–37.

Weinberg, N., Ouziel-Yahalom, L., Knoller, S., Efrat, S., and Dor, Y. (2007). Lineage tracing evidence for in vitro dedifferentiation but rare proliferation of mouse pancreatic beta-cells. Diabetes *56*, 1299–1304.

Wicksteed, B., Alarcon, C., Briaud, I., Lingohr, M.K., and Rhodes, C.J. (2003). Glucose-induced translational control of proinsulin biosynthesis is proportional to preproinsulin mRNA levels in islet beta-cells but not regulated via a positive feedback of secreted insulin. J. Biol. Chem. *278*, 42080–42090.

Wilson, D.S., Sheng, G., Jun, S., and Desplan, C. (1996). Conservation and diversification in homeodomain-DNA interactions: a comparative genetic analysis. Proc. Natl. Acad. Sci. USA *93*, 6886–6891.

Yokoi, N., Kanamori, M., Horikawa, Y., Takeda, J., Sanke, T., Furuta, H., Nanjo, K., Mori, H., Kasuga, M., Hara, K., et al. (2006). Association studies of variants in the genes involved in pancreatic beta-cell function in type 2 diabetes in Japanese subjects. Diabetes *55*, 2379–2386.

Zhu, X., Orci, L., Carroll, R., Norrbom, C., Ravazzola, M., and Steiner, D.F. (2002). Severe block in processing of proinsulin to insulin accompanied by elevation of des-64,65 proinsulin intermediates in islets of mice lacking prohormone convertase 1/3. Proc. Natl. Acad. Sci. USA *99*, 10299–10304.

Zito, E., Chin, K.T., Blais, J., Harding, H.P., and Ron, D. (2010). ERO1-beta, a pancreas-specific disulfide oxidase, promotes insulin biogenesis and glucose homeostasis. J. Cell Biol. *188*, 821–832.

Cell PRESS
Open ACCESS

EXTENDED EXPERIMENTAL PROCEDURES

Glucose Tolerance Tests, Insulin, and Proinsulin Measurements

For glucose tolerance tests, mice were fasted overnight for 16 hr and blood glucose levels were recorded (Bayer Contour glucometer; Bayer, Tarreytown, NJ) before an intraperitoneal injection of a 1.5mg/g body weight dextrose solution in sterile water. Blood glucose levels were recorded at 20, 40, 60, 90, 120, and 150 min after injection. Cohorts of at least six mice of the same sex per genotype were used to perform glucose measurements. To measure plasma insulin levels, mice were fasted overnight and blood was collected from tails into low retention microcentrifuge tubes (Eppendorf) before and 5 and 30 min after an intraperitoneal glucose injection. Collected blood was then centrifuged and serum was removed to assay for insulin using an insulin (mouse) ultrasensitive ELISA (ALPCO). To determine pancreatic insulin content, mice were fasted for four hours before whole pancreata were homogenized in 4 ml of a 2% acid:80% ethanol solution. Clarified samples were diluted 1:3000 in PBS before performing a mouse insulin ELISA (ALPCO). Insulin content was normalized to the protein concentration of pancreatic lysates (Pierce). To determine pancreatic proinsulin content, acid/ethanol extracts were diluted 1:1000 in PBS, measured by a mouse proinsulin ELISA (ALPCO) and values normalized to protein concentration. To determine the insulin to proinsulin ratio of pancreata, normalized proinsulin and insulin measurements were compared within each biological sample.

Islet Isolations and GSIS

Islet isolations were performed as previously described (Schaffer et al., 2011). Briefly, Liberase TL (Roche) was perfused into pancreata at a working concentration of 0.655 units/mL through the common hepatic bile duct. Pancreata were then removed and dissociated at 37°C for 15 min. Islets were separated onto a gradient composed of HBSS (Cellgro) and Histopaque (Sigma) layers. Purified islets were then hand picked twice under a dissection microscope to minimize acinar contamination.

For western blot analysis, islets were washed in sterile HBSS twice to remove residual BSA from islet isolations. For RNA isolation, islets were washed twice in DPBS (Calcium, magnesium, and RNase free) (Cellgro) and then lysed in buffer RLT (QIAGEN) containing beta-mercaptoethanol and stored in −80°C until RNA purification.

GSIS assays were performed as previously described (Schaffer et al., 2011). Briefly, islets were isolated from 6 mice per genotype and were incubated overnight in RPMI 1640 supplemented with 8mM glucose, 10% FBS, 2mM L-glutamine, 100u/mL Pen/Strep, 1mM sodium pyruvate, 10mM HEPES, and 0.25 μg/mL amphoterecin B. The next day, islets were washed and preincubated for 1 hr in a 2.7mM glucose solution. Afterward, groups of 10 islets were transferred to a 96 well dish into solutions of 2.7mM glucose, 16.7mM glucose, 30mM KCl with 2.7mM glucose, or 2 μM Bay K8644 with 16.7mM glucose. After incubation for 1 hr, supernatant was collected and islets were lysed overnight in a 2% acid:80% ethanol solution. Insulin was then measured in supernatants and lysates using a mouse insulin ELISA (ALPCO). Secreted insulin was calculated as percentage of total insulin content per hour.

ATP Measurement

ATP measurements were performed on isolated islets as described previously (Zhang et al., 2011). Briefly, on the day of islet isolation, isolated islets were equilibrated in RPMI 1640 supplemented with 2.7mM glucose for one hour. After incubation, 20 islet equivalents per mouse were washed in ice cold DPBS and subsequently lysed in 5% trichloroacetic acid (TCA) for 5 min at room temperature. TCA was then neutralized with 90 μl of 1% Triton X-100, 100mM Tris-Acetate pH 8.0. ATP levels were measured using the Enliten ATP assay kit (Promega, Madison, WI) and expressed as relative light units (RLU) per islet equivalent.

Incubation of Islets with Chemical Compounds

Mouse islets were isolated and washed in RPMI 1640 supplemented with 2.7mM glucose and 1% BSA. Islets were then incubated for three hours immediately after isolation in media supplemented with either a DMSO vehicle for control mice or 100nM recombinant insulin (Sigma), 60 μM +/− Bay K8644 (Sigma), or 10 μM glucokinase activator (EMD Calbiochem) for *Nkx6.1*$^{\Delta adult\beta}$ mice. After incubation, islets were washed in HBSS and lysed in 350 μl RLT containing beta-mercaptoethanol for subsequent RNA isolation.

Adenoviral Infection of Islets

Ad-Glut2 and *Ad-β-gal* viruses were kindly provided by C. Newgard (Duke University). Adenoviruses were expanded, purified, and titered as plaque forming units (PFU) per mL by ViraQuest Inc. Adenoviral infection of dispersed islets was adapted from a previously described protocol (Fiaschi-Taesch et al., 2009). Briefly, on the day of islet isolation, islets were dispersed in 0.05% Trypsin/EDTA (Invitrogen) with gentle agitation for 5 min at 37°C, washed in RPMI 1640 containing 10% FBS, and allowed to adhere overnight in 6 well tissue culture treated dishes coated with poly-l-lysine (Sigma Aldrich). 300 islet equivalents (~1000 cells per islet) pooled from two mice were used per biological sample for infections. On the day of infection, media was replaced with RPMI 1640 containing 2% FBS and islets were infected with a viral MOI of 100 (100 PFU/cell) for 2 hr before cells were washed and media was replaced with RPMI containing 10% FBS. 72 hr after viral infection, RNA was harvested from infected islets as described or immunofluorescence staining was performed as described on dispersed islets plated on poly-l-lysine coated coverslips (BD).

For determination of proinsulin and insulin content 72 hr after viral infection, dispersed islets were equilibrated in RPMI 1640 supplemented with 2.7mM glucose for 1 hr at 37°C. Media was then replaced with RPMI 1640 supplemented with 16.7mM glucose for

2 hr at 37°C. After incubation, dispersed islets were washed in ice cold DPBS (Ca^{2+} and Mg^{2+} free) followed by extraction of proinsulin and insulin with a 2% acid:80% ethanol solution. Proinsulin and insulin content was measured by ELISA (Alpco) and normalized by protein concentration determined by BCA (Pierce).

Electron Microscopy

For electron microscopy sample preparation, a fixative containing 2% paraformaldehyde, 2.5% glutaraldehyde, 3 μM $CaCl^2$ prepared in 0.1M sodium cacodylate buffer to a final pH 7.4 was used. Pancreata were perfused through the common hepatic bile duct with 200 μl of fixative before being removed from the mice. Pancreata were then immersed in fixative and islets were microdissected using fine razors at room temperature. Samples were incubated in fixative for at least 4 hr at 4°C, postfixed in 1% osmium tetroxide in 0.15 M cacodylate buffer for 1 hr and stained en bloc in 1% uranyl acetate for 1 hr. Samples were dehydrated in ethanol, embedded in Durcupan epoxy resin (Sigma-Aldrich), sectioned at 50 to 60 nm, and picked up on Formvar and carbon-coated copper grids. Sections were then stained with 2% uranyl acetate for 5 min and Sato's lead stain for 1 min. Grids were viewed using a Tecnai G2 Spirit BioTWIN transmission electron microscope equipped with an Eagle 4k HS digital camera (FEI, Hilsboro, OR). To quantify vesicle diameter, a total of 300 vesicles in 10 image planes were randomly selected for measurement. Vesicle diameter was measured as the longest distance between two points of a vesicle containing a mature insulin granule. To quantify vesicle number per area, blood vessel area was subtracted from total area, and vesicle numbers were quantified on at least 10 randomly selected 2900x image planes. To quantify vesicle subtype, total vesicle numbers were quantified on at least 10 randomly selected 2900x image planes and vesicles classified as either immature or mature were calculated as a percentage of total vesicles. At least 50 beta cells and 4000 vesicles were analyzed per genotype.

Immunohistochemistry and Morphometric Analysis

Mouse pancreata were fixed in 4% paraformaldehyde (Fisher Scientific) at 4°C overnight. After fixation, samples were washed three times with PBS and then incubated in 30% sucrose at 4°C overnight. Pancreata were embedded with Optimal Cutting Temperature Compound (O.C.T) (Tissue-Tek), frozen, and sectioned at 10 μm using a Cryostat (Leica). Sections were washed with PBS for 30 min and permeabilized in 0.15% Triton X-100 in PBS for 1 hr. For detection of nuclear antigens, antigen retrieval was performed at 37°C in 10 mM sodium citrate buffer, pH 6. For detection of Cyclin D2, adult pancreata were embedded in paraffin and subjected to antigen retrieval using a BioCare pressure cooker as previously described (Salpeter et al., 2011). Primary and secondary antibodies are listed in Tables S4 and S5, respectively. Immunodetection of p-AMPK required amplification of the primary signal using the TSA Kit (Invitrogen, Carlsbad, CA, USA). Staining using mouse primary antibodies was conducted using the mouse on mouse (M.O.M.) kit (Vector Labs) in conjunction with streptavidin/biotin blocking (Vector Labs) and streptavidin-conjugated secondary antibodies. When necessary, nuclei were counterstained with DAPI (Sigma) at 0.1 μg/ml. Images were captured using a Zeiss Axio Observer Z1 microscope with an apotome module on Zeiss AxioVision 4.8 and figures were prepared with Adobe Photoshop and Illustrator CS5.1.

Endocrine cell mass and area measurements were performed as previously described (Schaffer et al., 2011). Briefly, immunohistochemistry for insulin or chromogranin A was performed on six evenly spaced sections throughout the entire pancreas. To calculate endocrine cell mass, tiled images were taken from each section, fluorescent area for chromogranin A was determined as a percentage of the total pancreatic area (ImagePro Plus 5.0.1), and multiplied by the weight of the pancreas. To determine the percentage of endocrine cells expressing insulin, the total number of $insulin^+chromogranin\ A^+$ cells was divided by the total number of $chromogranin\ A^+$ cells. For examination of apoptosis, TUNEL analysis was performed as specified by the manufacturer (Millipore). For all quantifications, at least 50 islets were examined per mouse.

Analysis of Proliferation after Treatment with Bay K8644

To examine beta cell proliferation after administration of Bay K8644, mice were administered 8mg/kg Bay K8644 dissolved in 20% DMSO, 79% Salene, and 1% Tween 80 or vehicle control (Salpeter et al., 2011). Pancreata were harvested 24 hr after injection and processed for immunostaining.

Western Blot Analysis

To determine Cyclin D2 and Neurogenin 3 protein levels, islets were lysed in RIPA buffer and 30 μg of protein was loaded onto a 10% Tris-HCl SDS- polyacrylamide gel. Protein was then transferred to a nitrocellulose membrane and membranes were blocked in 5% milk PBS/0.1% tween followed by incubation with primary antibodies in blocking solution overnight at 4°C and secondary antibodies for 1 hr at room temperature the following day. Primary and secondary antibodies are listed in Tables S4 and S5, respectively.

Microarray Analysis and Statistical Methods

To identify Nkx6.1-regulated genes in islets, we isolated islets from six mice per genotype four days after the final tamoxifen injection and then pooled islets from two mice per genotype for a total of three independent biological replicates. Each individual RNA sample was prepared as per the manufacturer's instructions (QIAGEN Micro RNeasy isolation kit). RNA was quantified using a NanoDrop-1000 spectrophotometer and quality was assessed with an Agilent 2100 Bioanalyzer (Agilent Technologies, Santa Clara, CA). Approximately 150 ng of total RNA was amplified and labeled with Cy3 using the QuickAmp Low Input Labeling Kit, One-Color (Agilent Technologies). This labeling reaction produced 1650 ng of Cy3-labeled cRNA (anti-sense), by first converting mRNA primed with

an oligo (d)T-T7 primer into dsDNA with MMLV-RT. The sample was then amplified using T7 RNA Polymerase in the presence of Cy3-CTP. Three independent biological samples of each genotype were hybridized to Agilent Whole Mouse Genome Oligo Microarray G2519F chips. Agilent microarray and data analysis was performed with support from the UCSD BioMedical Genomics Microarray (BIOGEM) Facility (San Diego, CA). Expression changes were considered significant if they had a false discovery rate (FDR) less than 0.01 and a fold change of at least 1.5. A table of significantly changed genes is provided in Table S1.

qRT-PCR

Total mRNA was purified from isolated islets from individual mice with the RNAeasy Micro kit (QIAGEN). Subsequent cDNA synthesis was performed using the iScript Reverse Transcription Supermix for RT-qPCR (BioRad). qPCR reactions were run in biological triplicates and in technical replicates with 0.5 to 5 ng cDNA per reaction. A CFX96 real-time system (BioRad) was used to acquire data from qRT-PCR reactions. The housekeeping gene *GAPDH*, verified to remain unchanged between samples from normalized microarray data, was used as an endogenous control. Primers used for verifications are listed in Table S6.

ChIP-Seq Analysis

Nkx6.1-enriched regions were identified with the findpeaks parameter from the HOMER package. A p value of 1e-4, peak size of 150, and a six-fold enrichment over input was used to compare Nkx6.1 ChIP reads to input reads for identification of significant Nkx6.1 binding peaks. Binding peaks were annotated with the gene with the nearest transcriptional start site within 10kb of an identified Nkx6.1 binding peak. To identify genes that were bound and regulated by Nkx6.1, the list of significantly changed genes in islets from *Nkx6.1*$^{\Delta adult\beta}$ mice was compared to the gene list of annotated peaks from the Nkx6.1 ChIP-seq experiment using BioVenn (Hulsen et al., 2008). To identify de novo Nkx6.1 binding motifs, the HOMER parameter findmotifsgenome.pl was used. Lists of annotated peaks and comparison of ChIP-seq and microarray data are provided in Tables S2 and S3.

SUPPLEMENTAL REFERENCES

Henseleit, K.D., Nelson, S.B., Kuhlbrodt, K., Hennings, J.C., Ericson, J., and Sander, M. (2005). NKX6 transcription factor activity is required for alpha- and beta-cell development in the pancreas. Development *132*, 3139–3149.

Zhang, Z., Wakabayashi, N., Wakabayashi, J., Tamura, Y., Song, W.J., Sereda, S., Clerc, P., Polster, B.M., Aja, S.M., Pletnikov, M.V., et al. (2011). The dynamin-related GTPase Opa1 is required for glucose-stimulated ATP production in pancreatic beta cells. Mol. Biol. Cell *22*, 2235–2245.

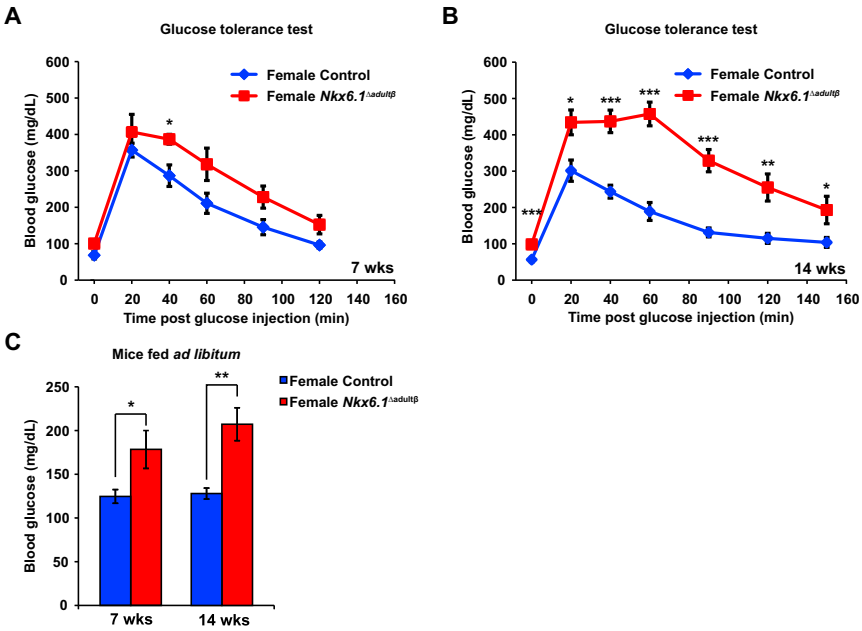

Figure S1. Female *Nkx6.1*$^{\Delta adult\beta}$ Mice Progress to Diabetes Less Rapidly than Males, Related to Figure 1

(A–C) Intraperitoneal glucose tolerance tests (A and B) and blood glucose measurements of mice fed *ad libitum* (C) reveal glucose intolerance in female *Nkx6.1*$^{\Delta adult\beta}$ mice at 14 wks (n = 6). wk, week. Data are shown as mean ± SEM. *p < 0.05, **p < 0.01, ***p < 0.001.

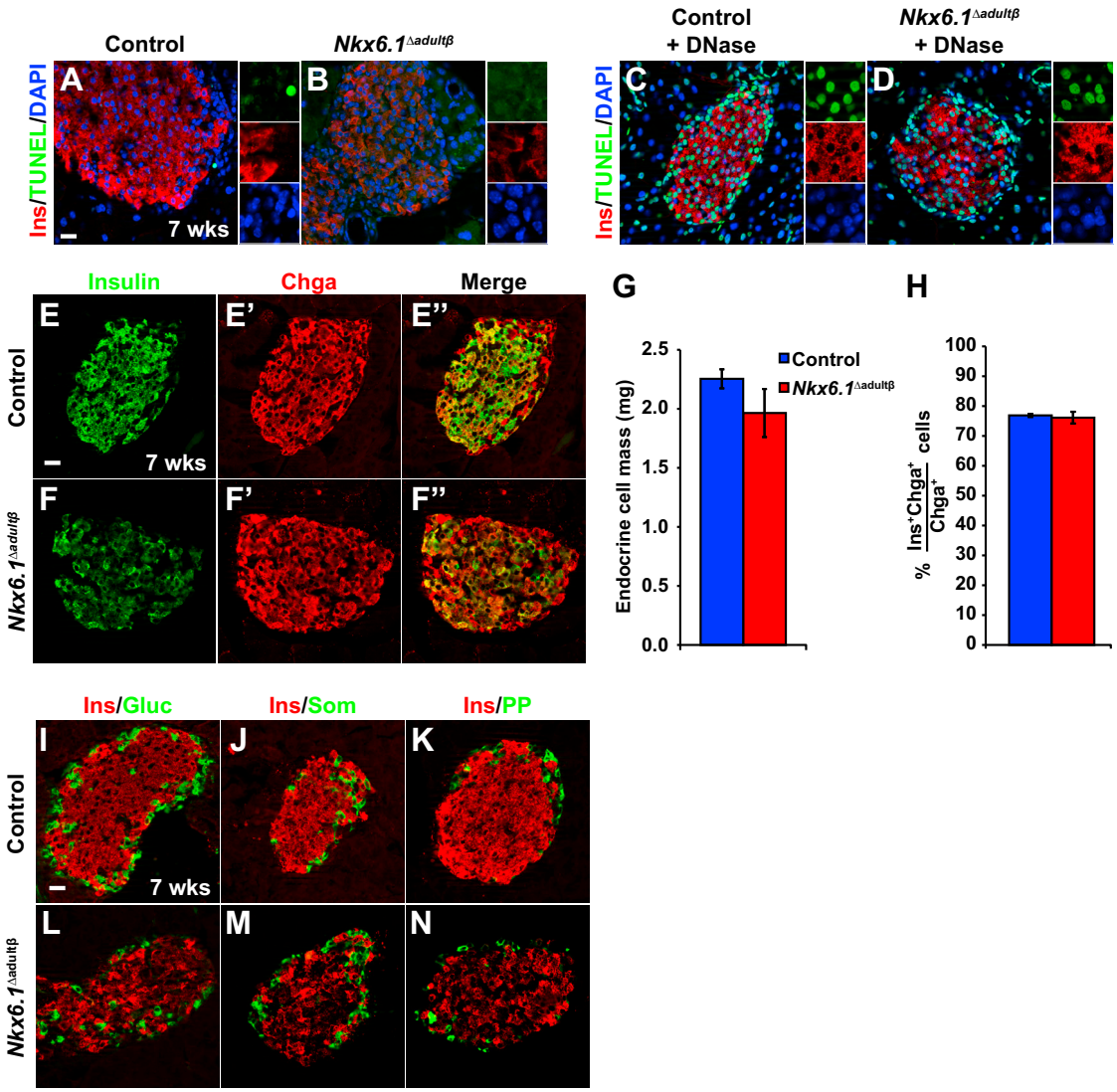

Figure S2. *Nkx6.1*$^{\Delta adult\beta}$ Mice Have Normal Beta Cell Viability, Pancreatic Endocrine Cell Mass, and Beta Cell Numbers, Related to Figure 1

(A–D) TUNEL assay combined with immunofluorescence staining for insulin and DAPI staining shows that beta cells in *Nkx6.1*$^{\Delta adult\beta}$ and control mice are not apoptotic at 7 wks. Pancreatic sections were treated with DNaseI as a positive control for the TUNEL assay (C and D). Right row shows higher magnification images and split color channels.

(E and F) Immunofluorescence staining for Chga and insulin in *Nkx6.1*$^{\Delta adult\beta}$ and control mice at 7 wks.

(G and H) Quantification of endocrine cell mass based on Chga staining (G) and insulin/Chga copositive relative to total Chga positive cell numbers (H) shows no difference between *Nkx6.1*$^{\Delta adult\beta}$ and control mice (n = 3).

(I–N) Immunofluorescence staining reveals that insulin-expressing cells do not coexpress glucagon, somatostatin, or pancreatic polypeptide in *Nkx6.1*$^{\Delta adult\beta}$ mice at 7 wks. Scale bar = 20 μm. Ins, insulin; TUNEL, terminal deoxynucleotidyl transferase dUTP nicked end labeling; DAPI, 4',6-diamidino-2-phenylindole; Chga, chromogranin A; Gluc, glucagon; Som, somatostatin; PP, pancreatic polypeptide; wk, week. Data are shown as mean ± SEM.

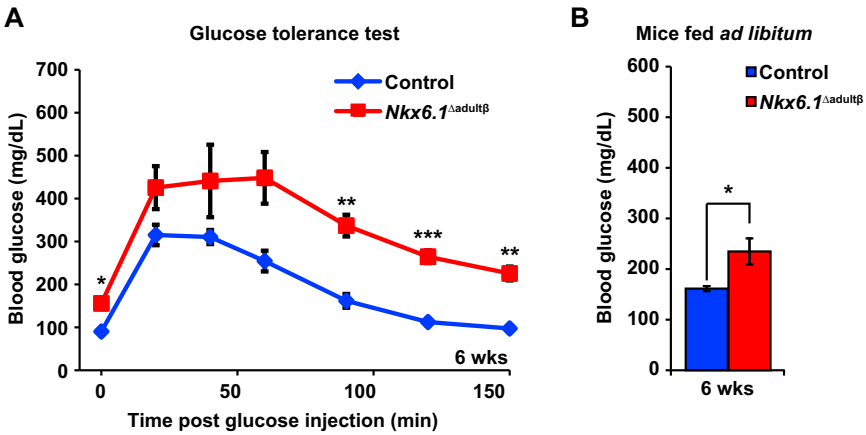

Figure S3. *Nkx6.1*$^{\Delta adult\beta}$ Mice Are Not Overtly Diabetic 1 Week after Completion of Tamoxifen-Mediated *Nkx6.1* Inactivation, Related to Figure 2

(A and B) Intraperitoneal glucose tolerance test (A) and random blood glucose measurements (B) in male *Nkx6.1*$^{\Delta adult\beta}$ and control mice at 6 weeks (wks) (n = 6). Data are shown as mean ± SEM. *p < 0.05, **p < 0.01, ***p < 0.001.

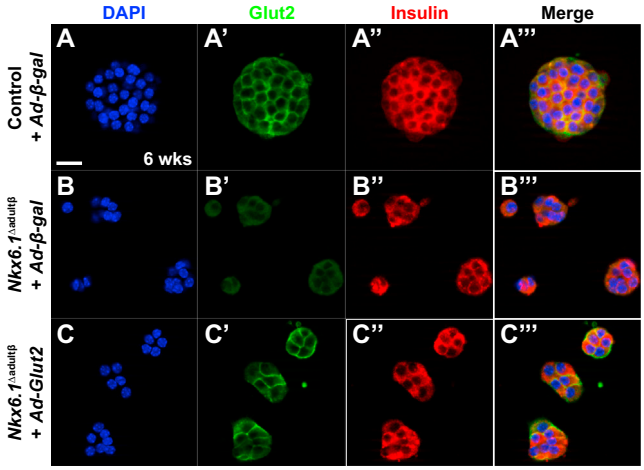

Figure S4. Glut2 Protein Expression Is Restored in *Nkx6.1*$^{\Delta adult\beta}$ Islets after Infection with *Glut2*-Expressing Adenovirus, Related to Figure 4

(A–C‴) Immunofluorescent staining of dispersed islets for DAPI, Glut2 and insulin after infection of *Nkx6.1*$^{\Delta adult\beta}$ and control islets with *Ad-Glut2* or *Ad-β-gal* reveals that Glut2 protein expression is restored in *Nkx6.1*$^{\Delta adult\beta}$ islets. Mice were 6 weeks (wks) old. Scale bar = 20 μm.

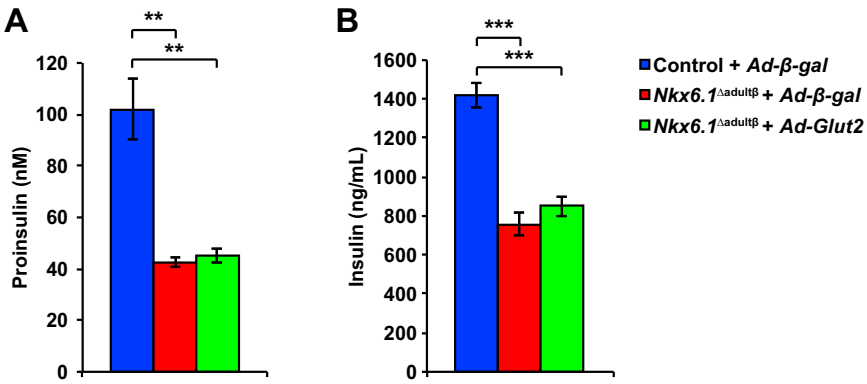

Figure S5. Expression of Glut2 in *Nkx6.1*$^{\Delta adult\beta}$ Islets Does Not Restore Proinsulin or Insulin Content, Related to Figure 5

(A and B) Measurements of proinsulin (A) and insulin content (B) after infection of *Nkx6.1*$^{\Delta adult\beta}$ and control islets with *Ad-Glut2* or *Ad-β-gal* shows that adenoviral expression of *Glut2* in *Nkx6.1*$^{\Delta adult\beta}$ islets does not increase either proinsulin or insulin levels (n = 6). Data are shown as mean ± SEM. **p < 0.01, ***p < 0.001.